Modifying the Internal Substituents of Self-Assembled Cages Controls their Molecular Recognition and Optical Properties

Connor Z. Woods, Hoi-Ting Wu, Courtney Ngai, Bryce da Camara, Ryan R. Julian and Richard J. Hooley*

Department of Chemistry, University of California-Riverside, Riverside, CA 92521, U.S.A.

Electronic Supplementary Information

Table of Contents

I. Characterization of Substrates and Products

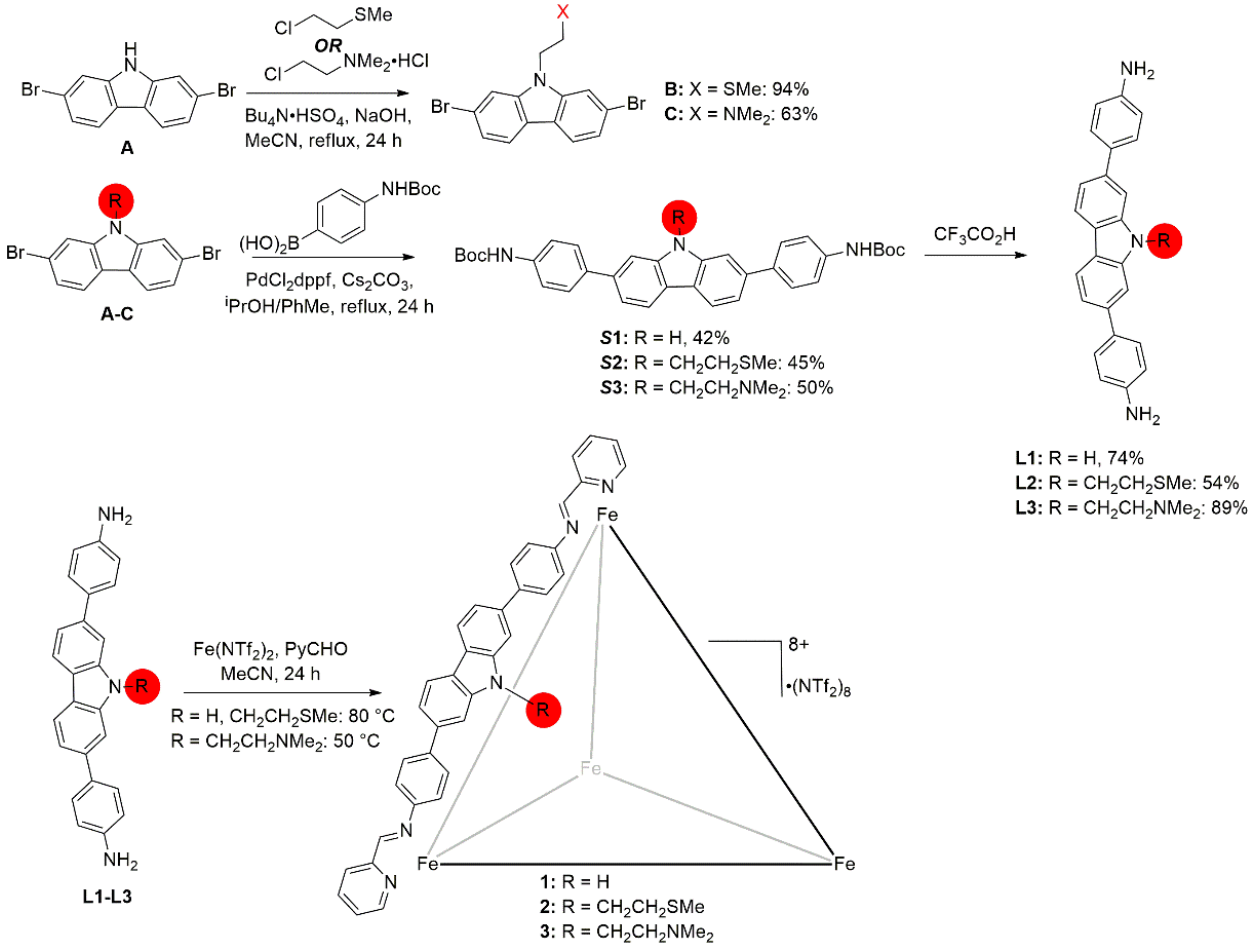

Figure *S-1*. Reaction scheme for the synthesis of cages **1-3**.

Unfunctionalized Cage 1:

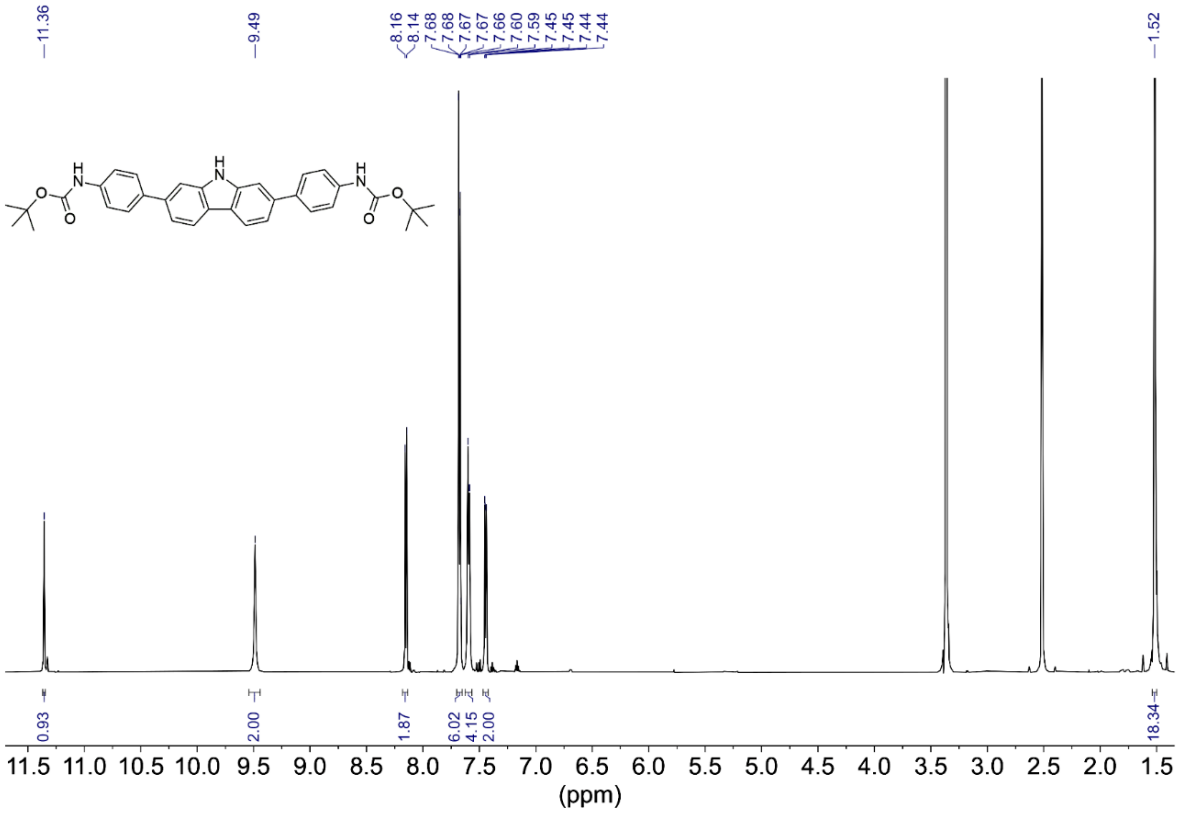

Figure *S-2*. ^{1}H NMR spectrum of ***S1*** (600 MHz, 298 K, DMSO-d_6).

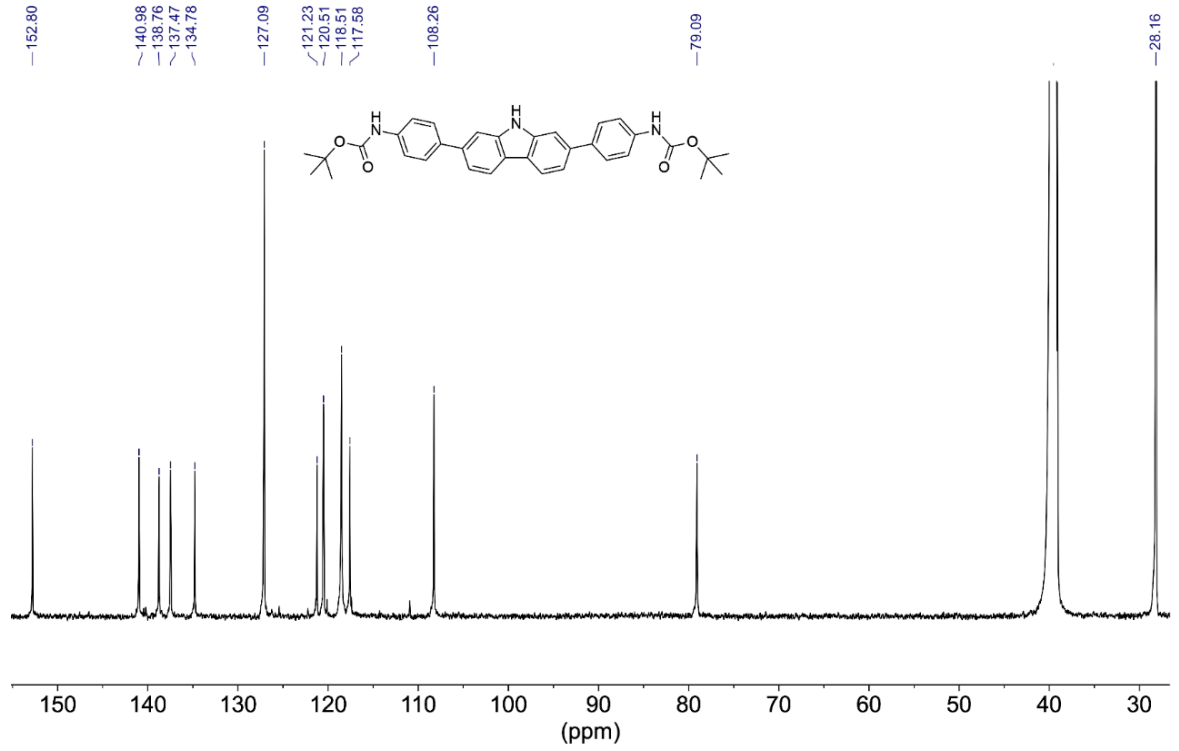

Figure *S-3*. ^{13}C NMR spectrum of ***S1*** (100 MHz, 298 K, DMSO-d_6).

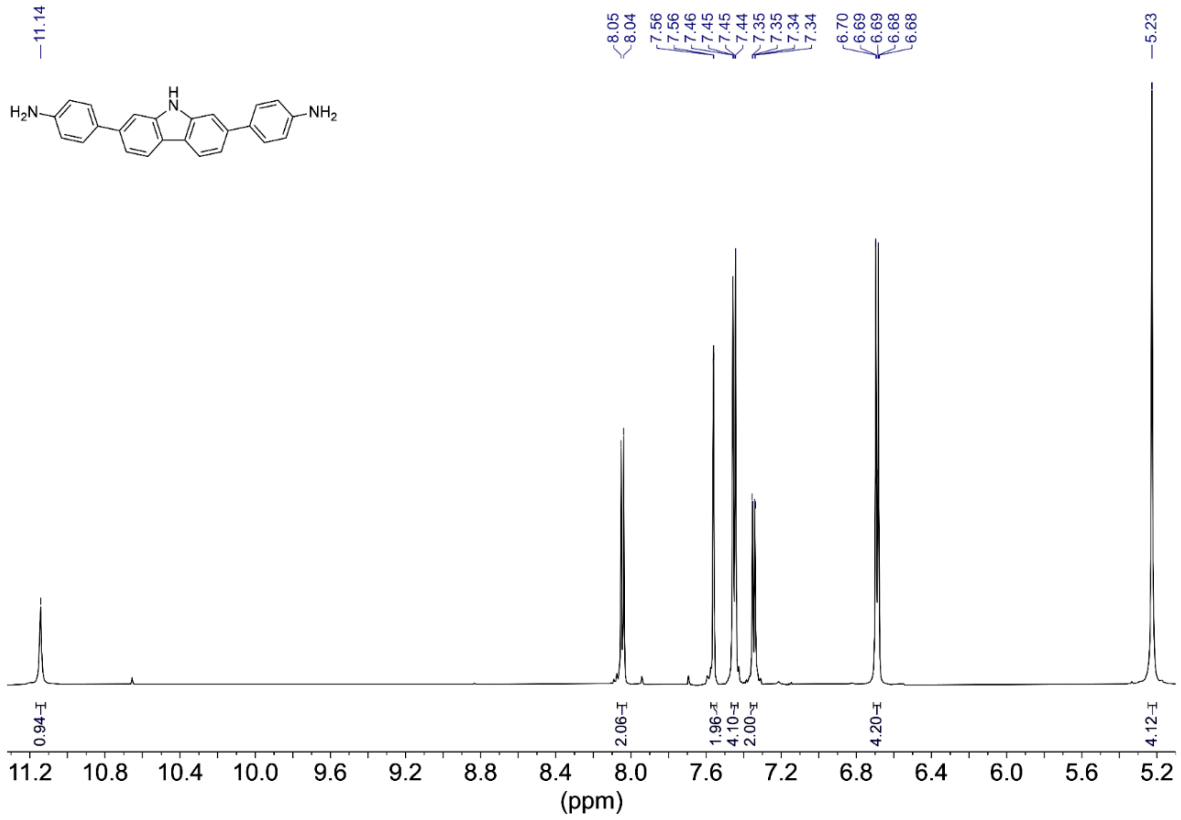

Figure *S*-4. ^{1}H NMR spectrum of **L1** (600 MHz, 298 K, DMSO-d_6).

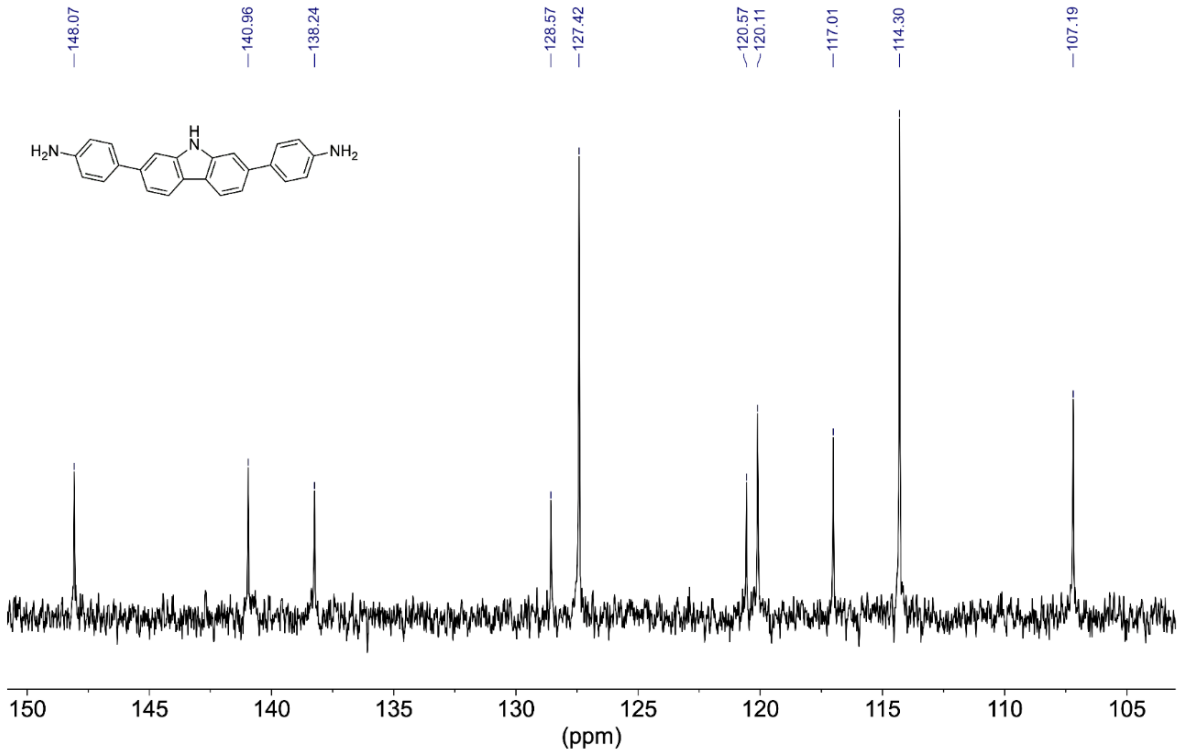

Figure *S*-5. ^{13}C NMR spectrum of **L1** (150 MHz, 298 K, DMSO-d_6).

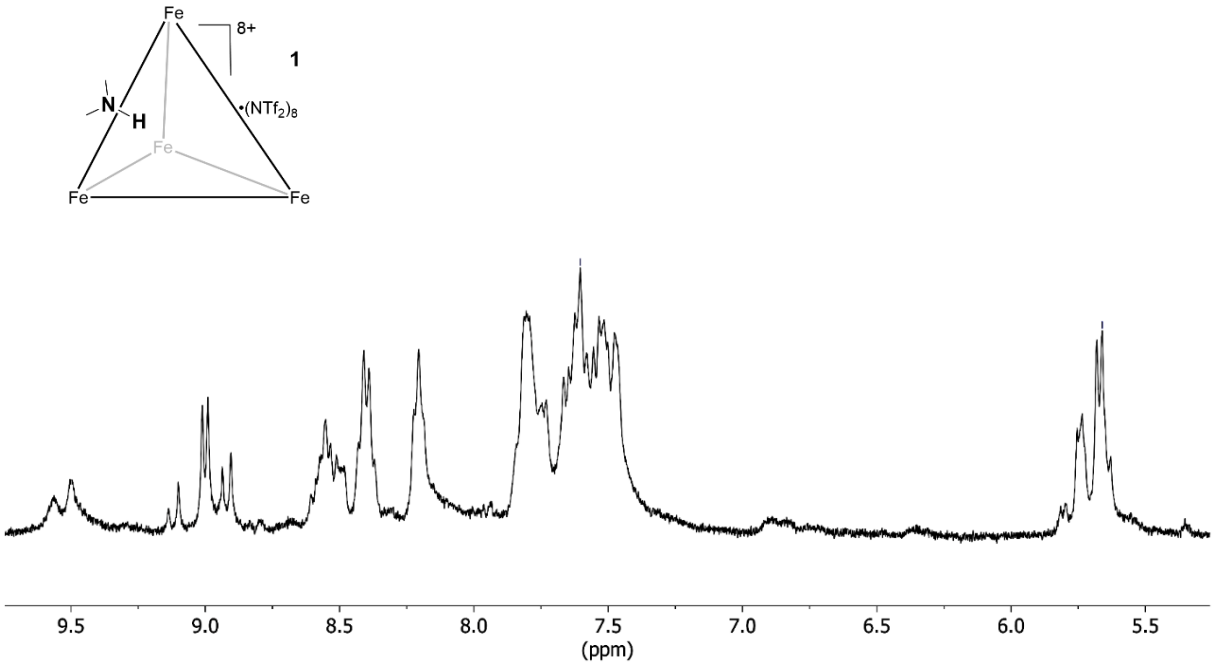

Figure *S-6*. ^{1}H NMR spectrum of **1** (400 MHz, 298 K, CD_3CN).

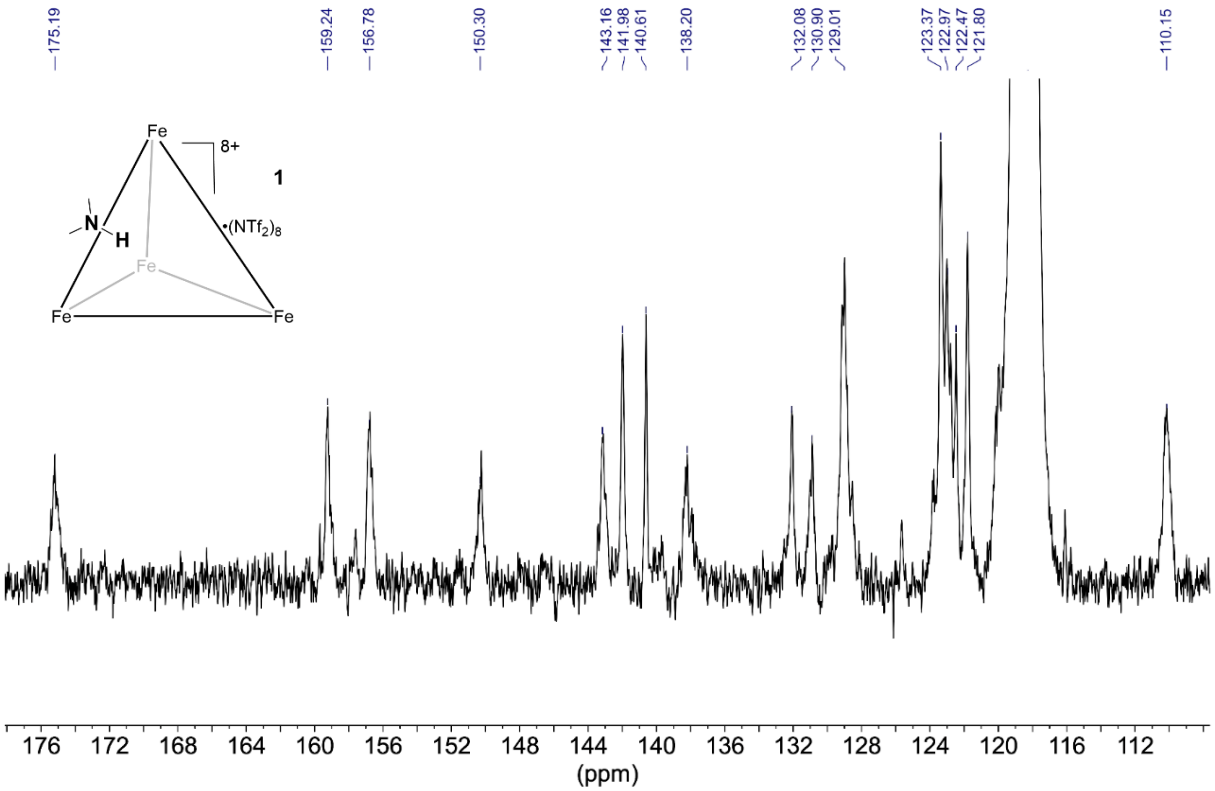

Figure *S-7*. ^{13}C NMR spectrum of **1** (100 MHz, 298 K, CD_3CN).

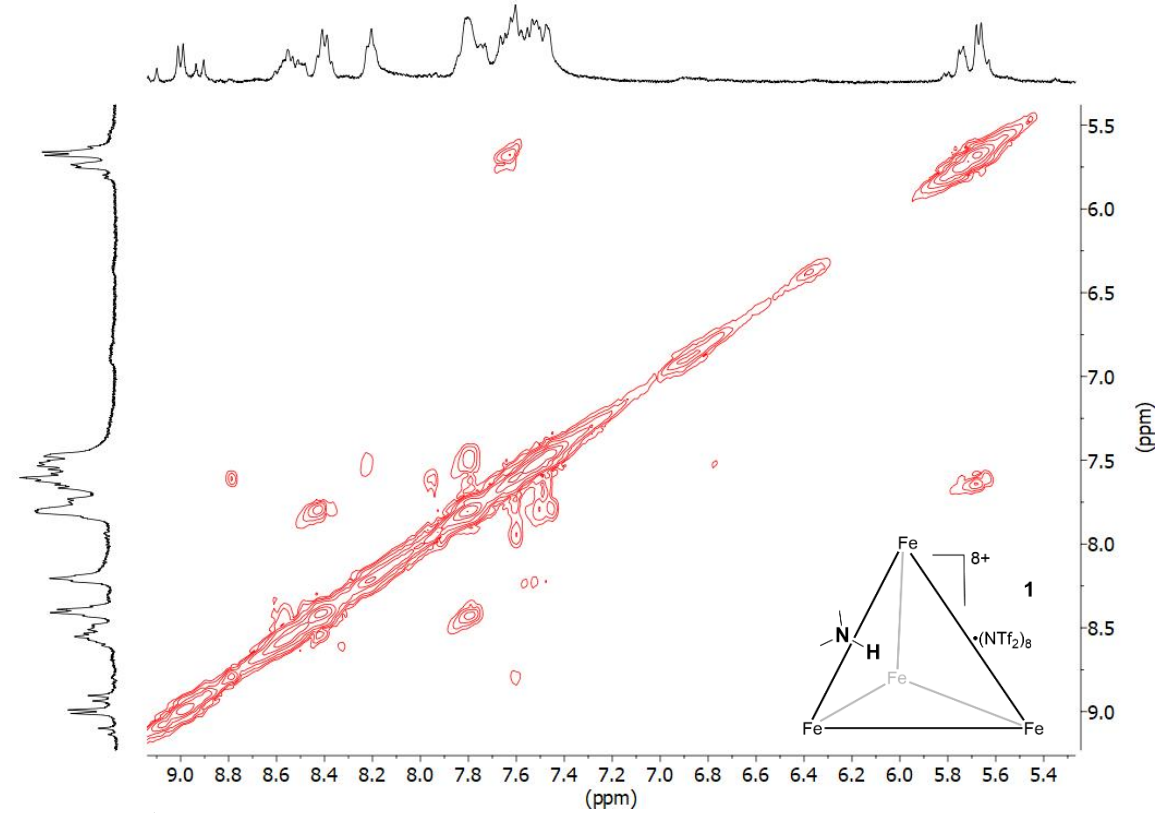

Figure *S*-*8*. ^{1}H COSY NMR spectrum of **1** (400 MHz, 298 K, CD_3CN).

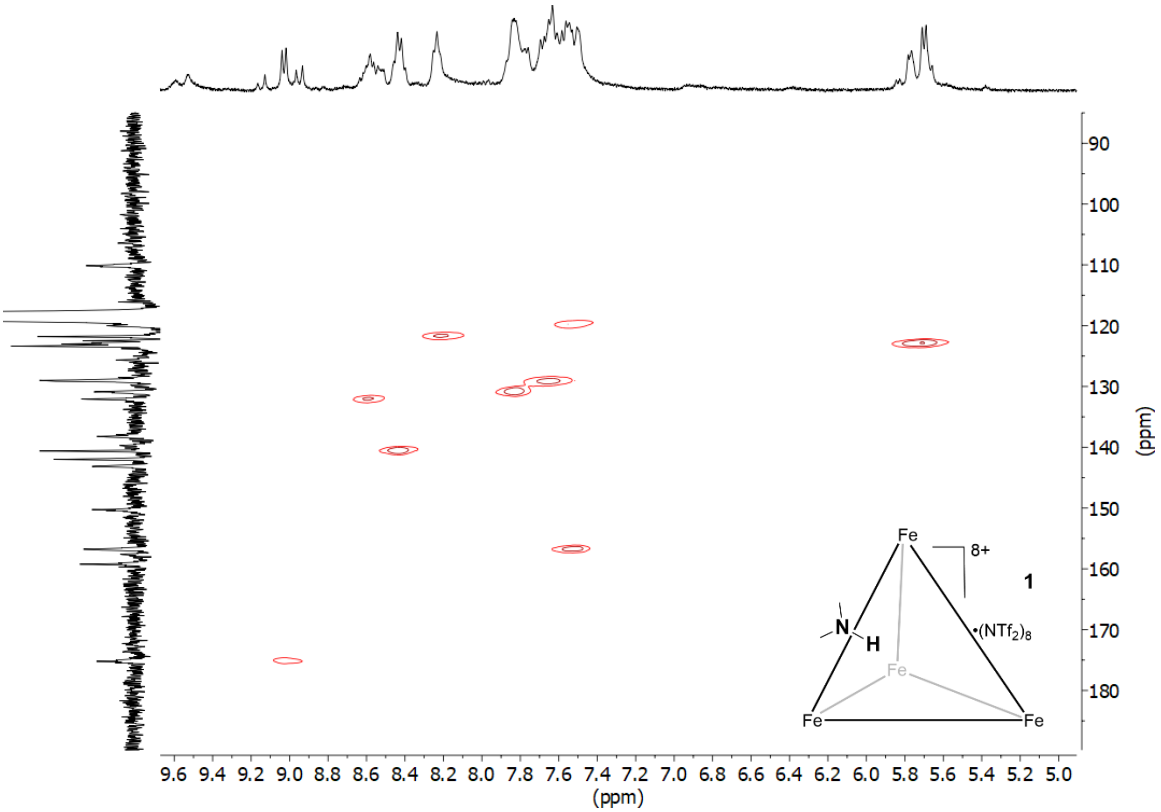

Figure *S*-*9*. HSQC NMR spectrum of **1** (400 MHz, 298 K, CD_3CN).

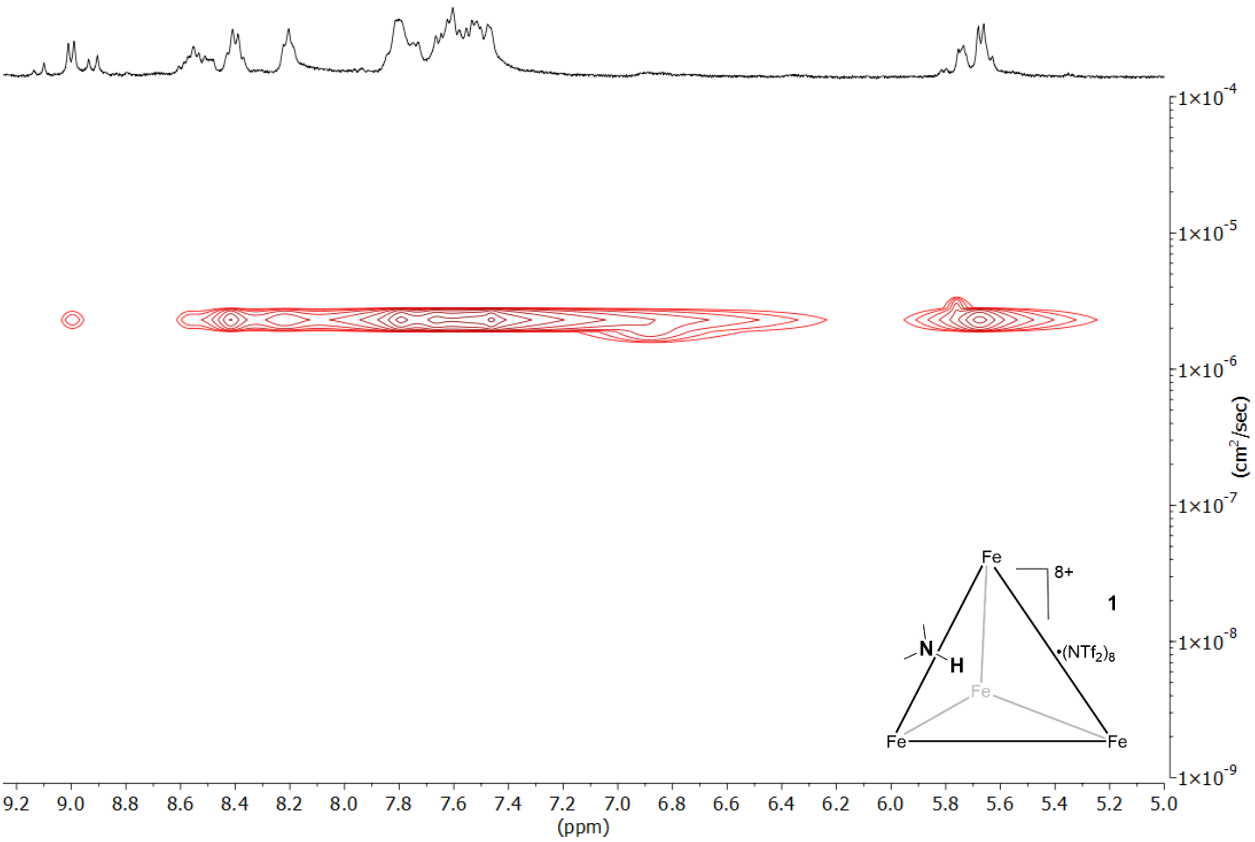

Figure *S-10*. DOSY NMR spectrum of **1** (600 MHz, 298 K, CD_3CN). Diffusion constant; 2.30 x 10^{-6} cm^2/sec.

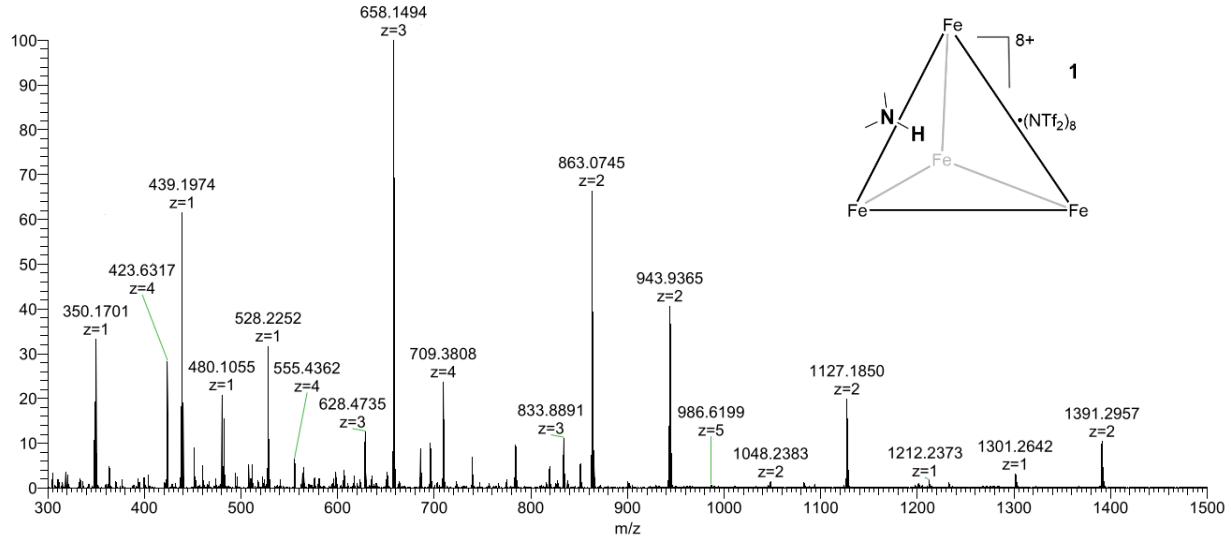

Figure *S-11*. Full mass spectrum of **1** (CH_3CN).

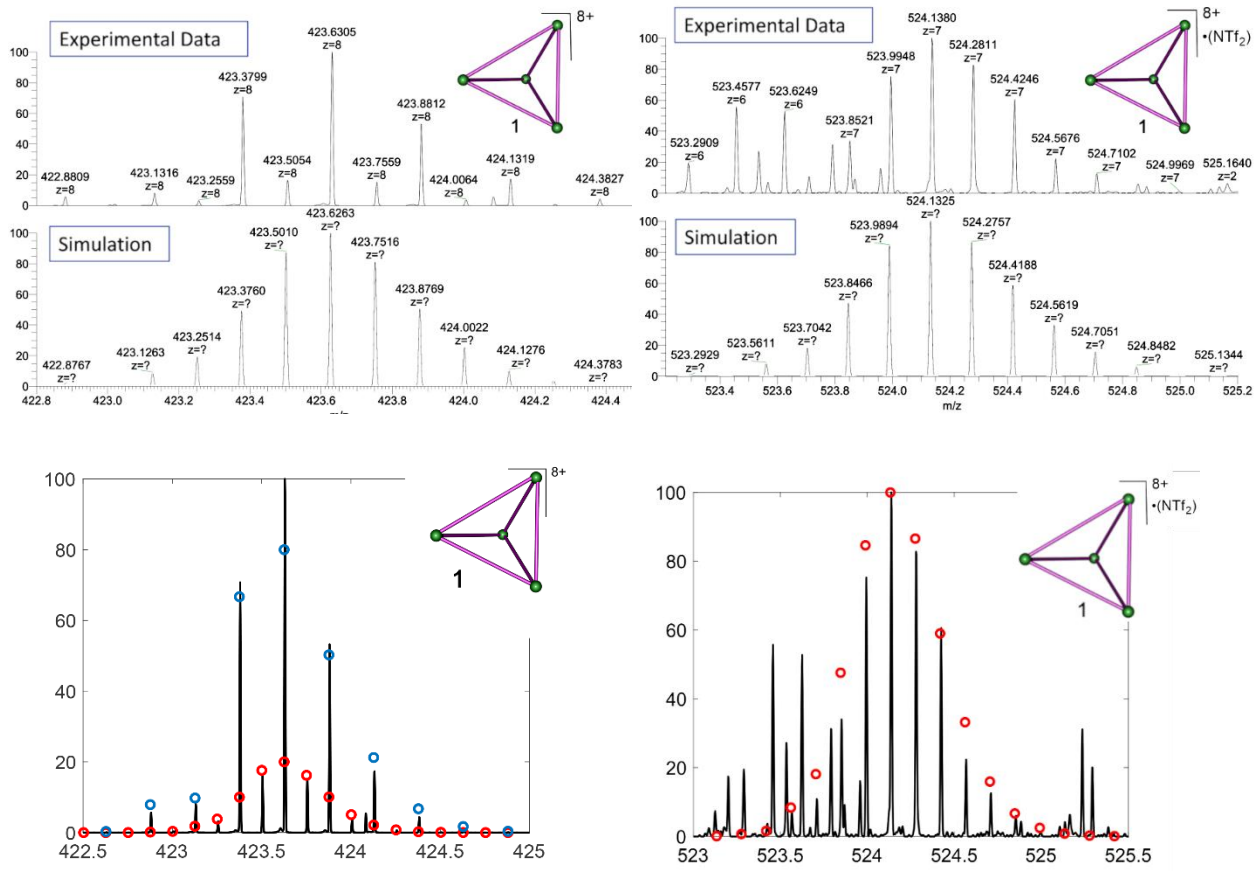

Figure *S-12*. Mass spectrum of predicted ions $[\mathbf{1}]^{8+}$ and $[\mathbf{1}\bullet 1NTf_2]^{7+}$ stacked versus predicted peaks.

Thioether Cage 2:

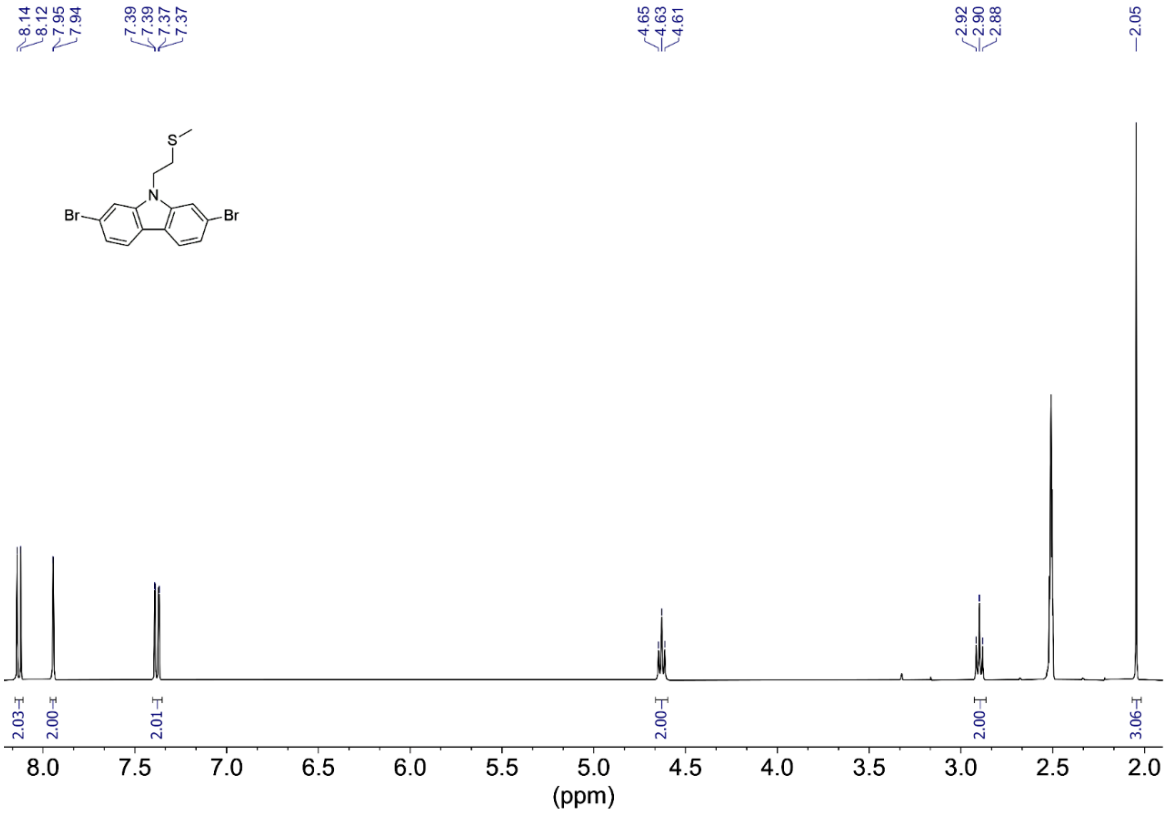

Figure *S-13* ^{1}H NMR spectrum of **B** (400 MHz, 298 K, DMSO-d_6).

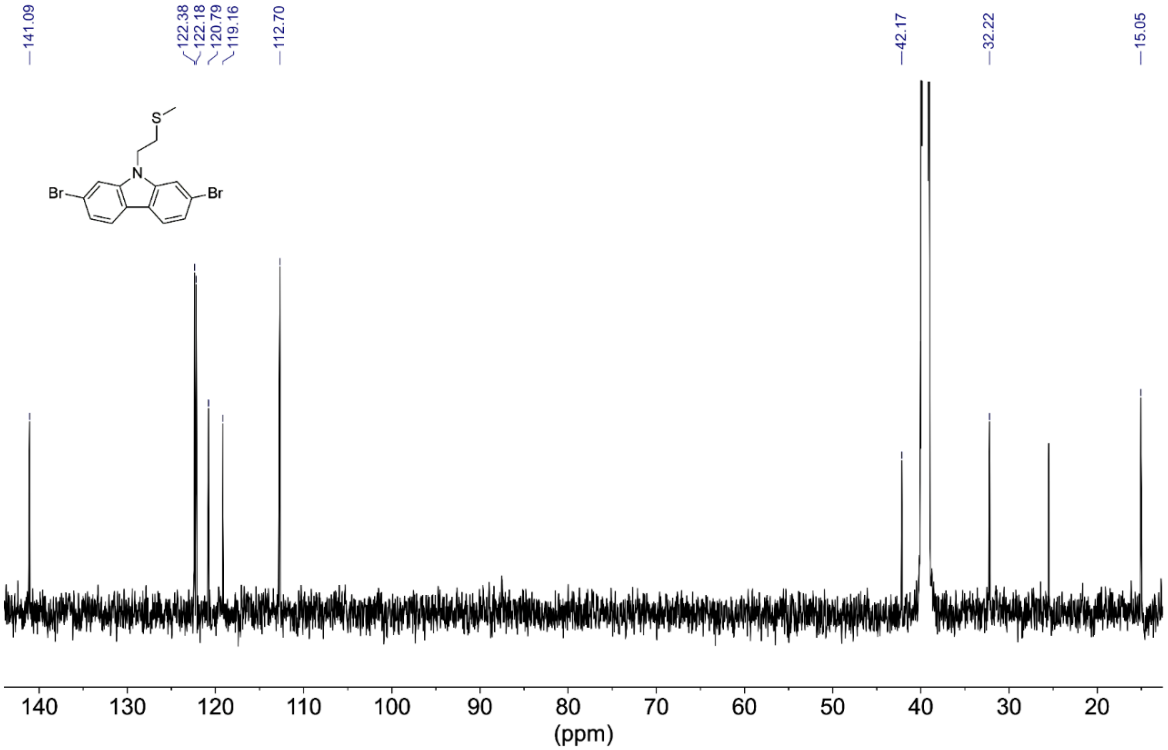

Figure *S-14*. ^{13}C NMR spectrum of **B** (100 MHz, 298 K, DMSO-d_6).

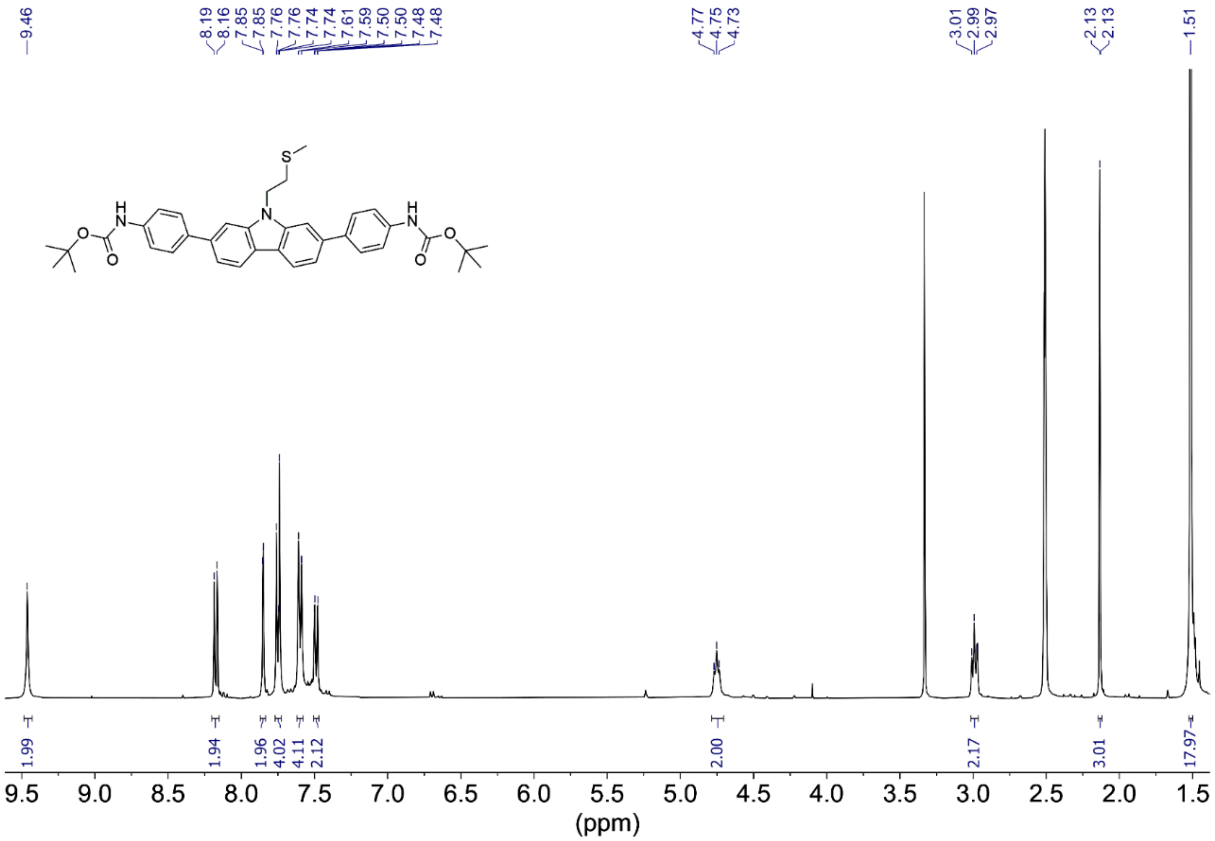

Figure *S-15*. ^{1}H NMR spectrum of ***S2*** (400 MHz, 298 K, DMSO-d_6).

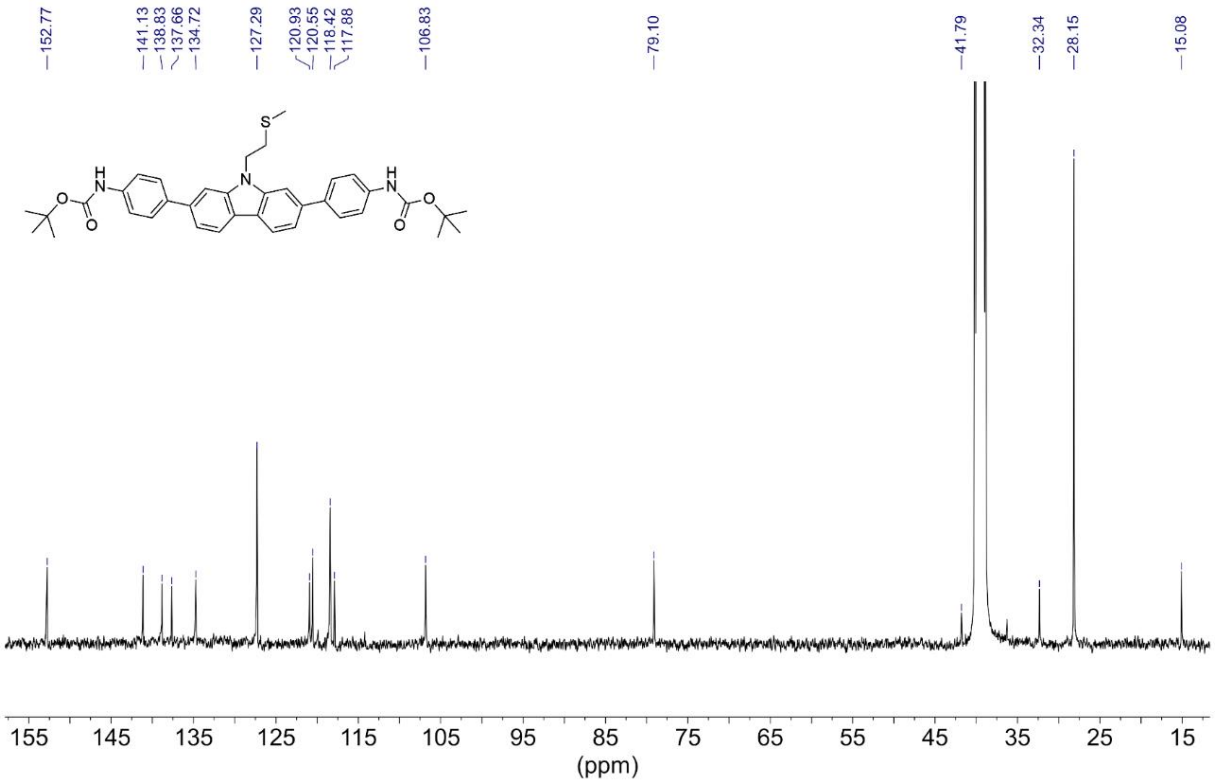

Figure *S-16*. ^{13}C NMR spectrum of ***S2*** (150 MHz, 298 K, DMSO-d_6).

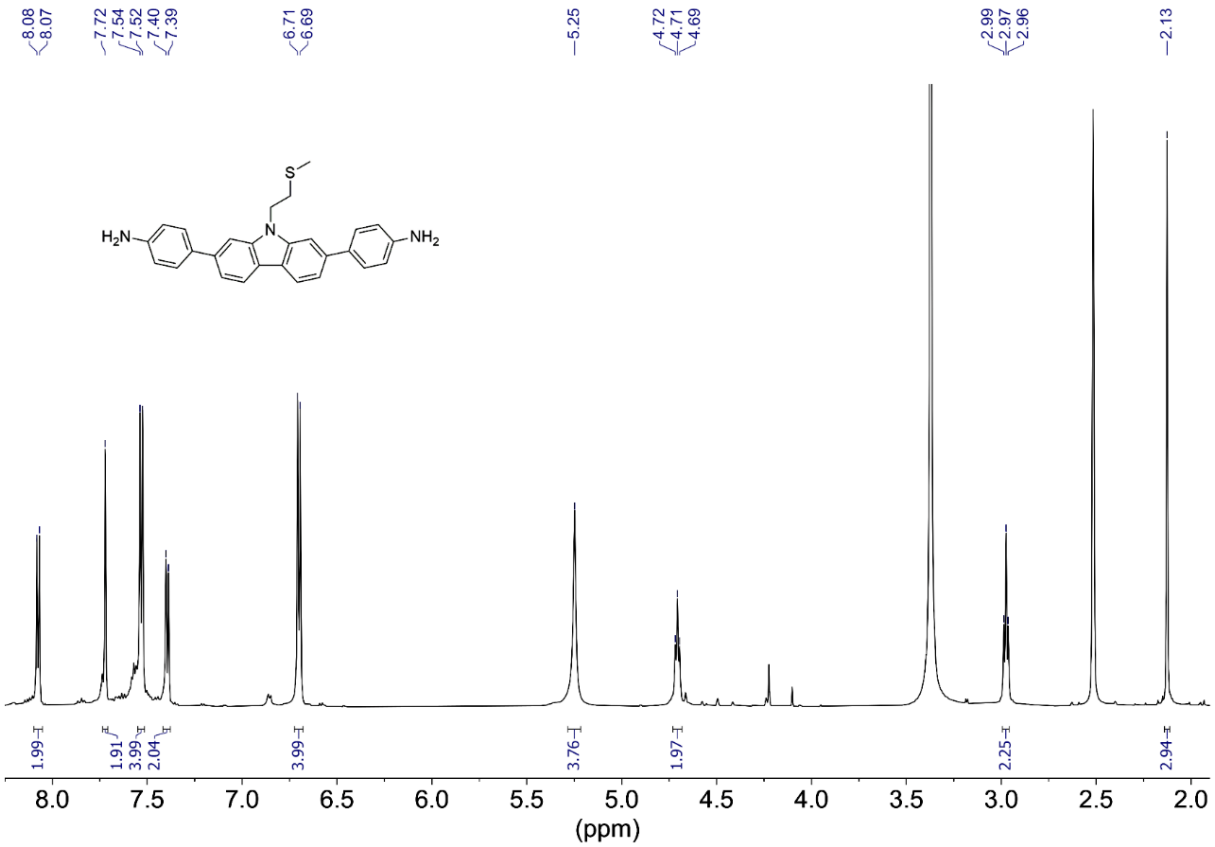

Figure *S-17.* ^{1}H NMR spectrum of **L2** (600 MHz, 298 K, DMSO-d_6).

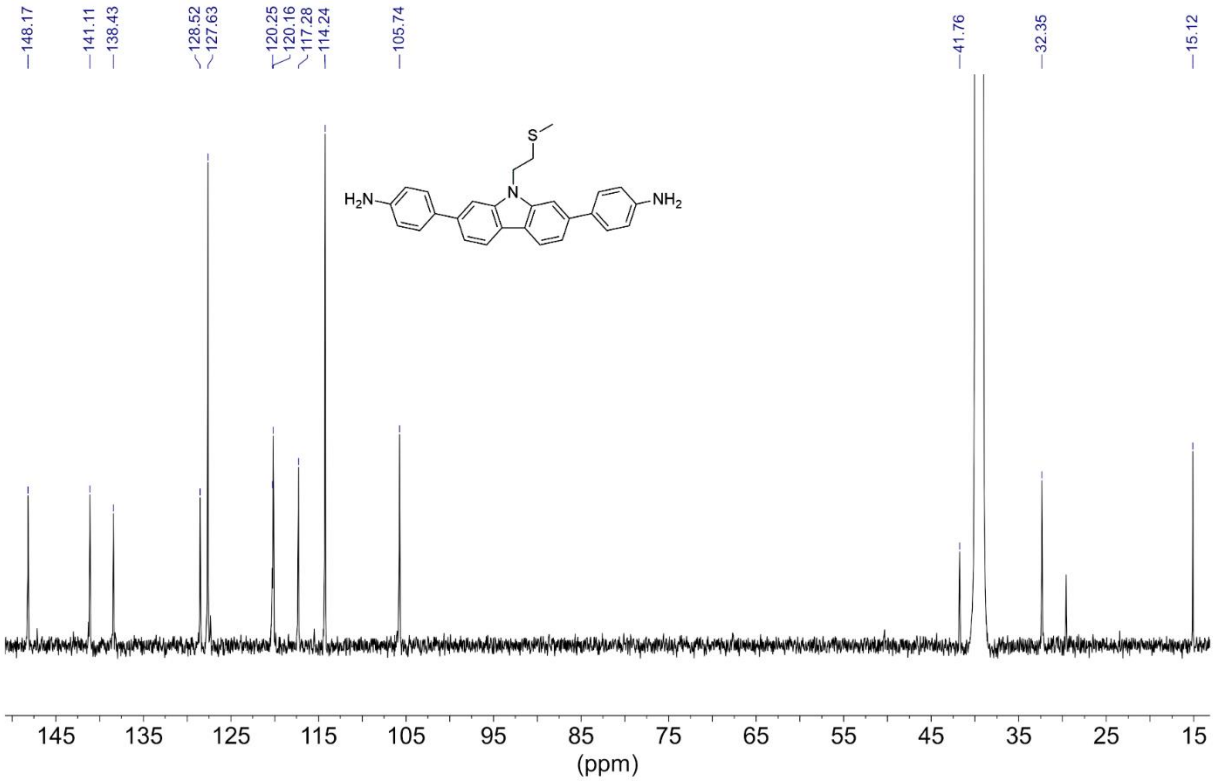

Figure *S-18.* ^{13}C NMR spectrum of **L2** (150 MHz, 298 K, DMSO-d_6).

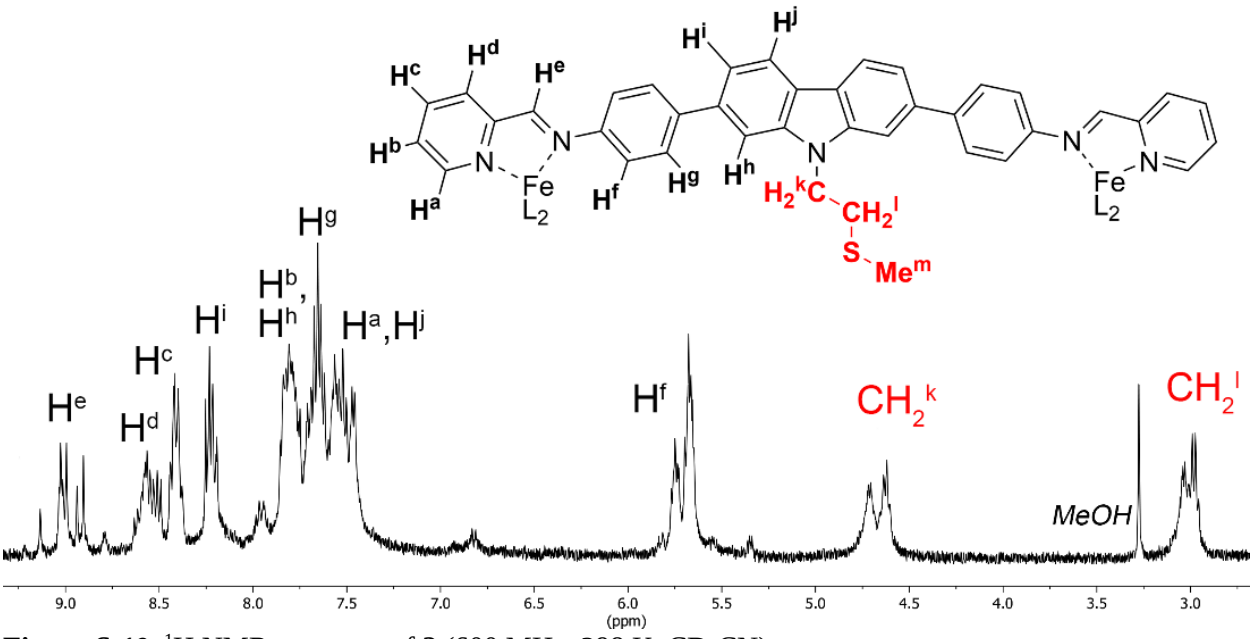

Figure *S-19*. ^{1}H NMR spectrum of **2** (600 MHz, 298 K, CD_3CN).

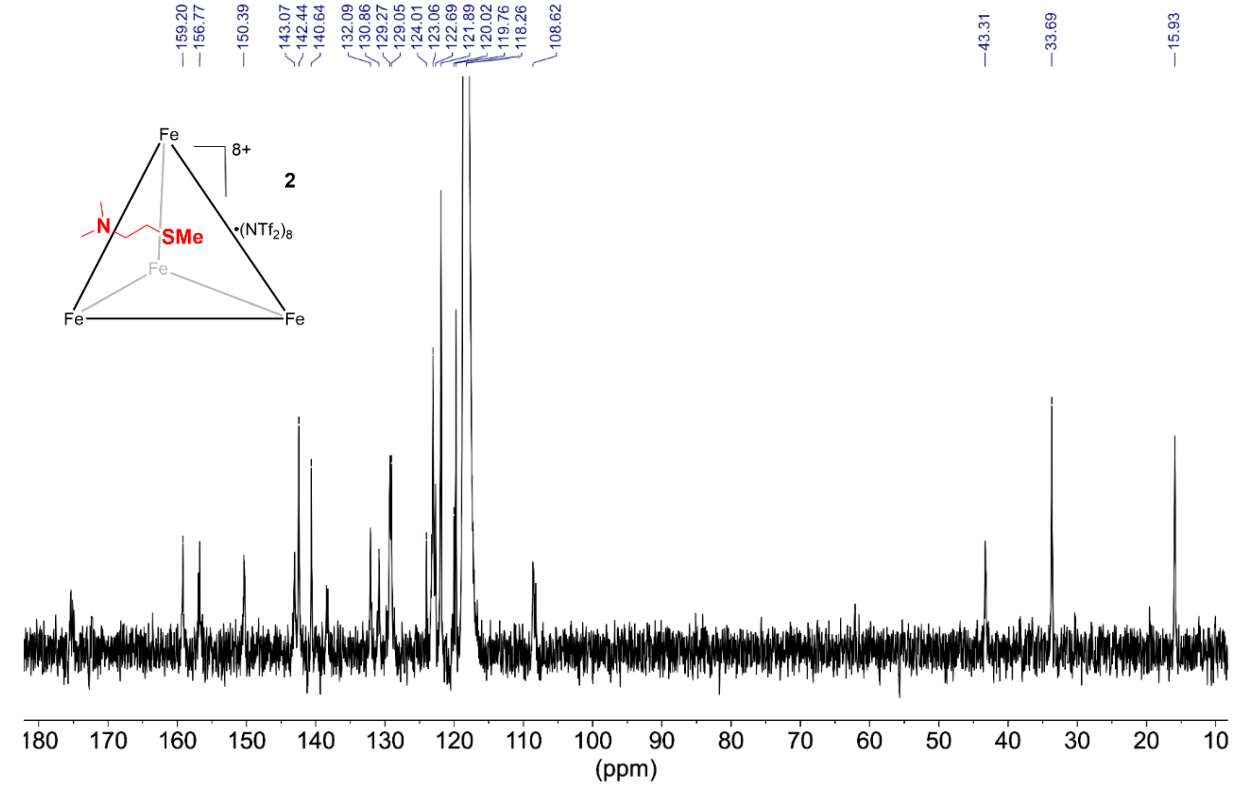

Figure *S-20*. ^{13}C NMR spectrum of **2** (150 MHz, 298 K, DMSO-d_6).

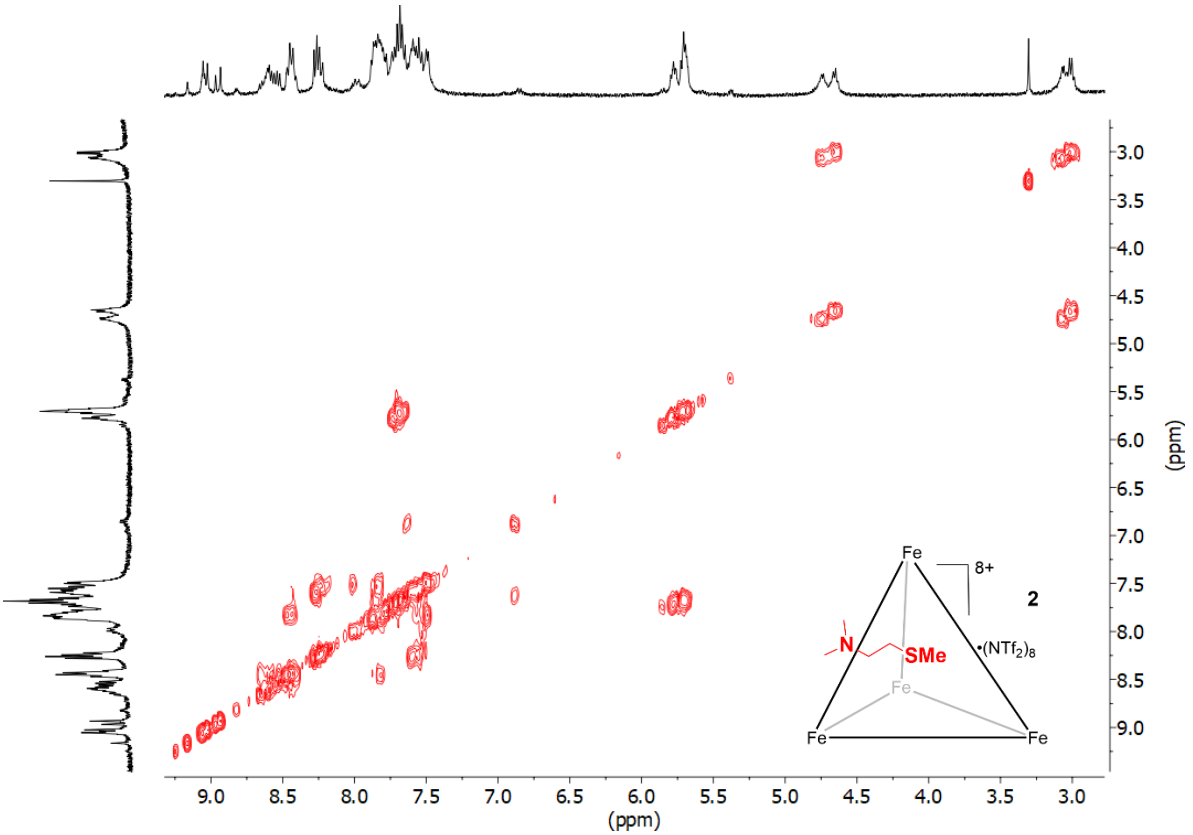

Figure *S-21*. ^{1}H COSY NMR spectrum of **2** (600 MHz, 298 K, CD_3CN).

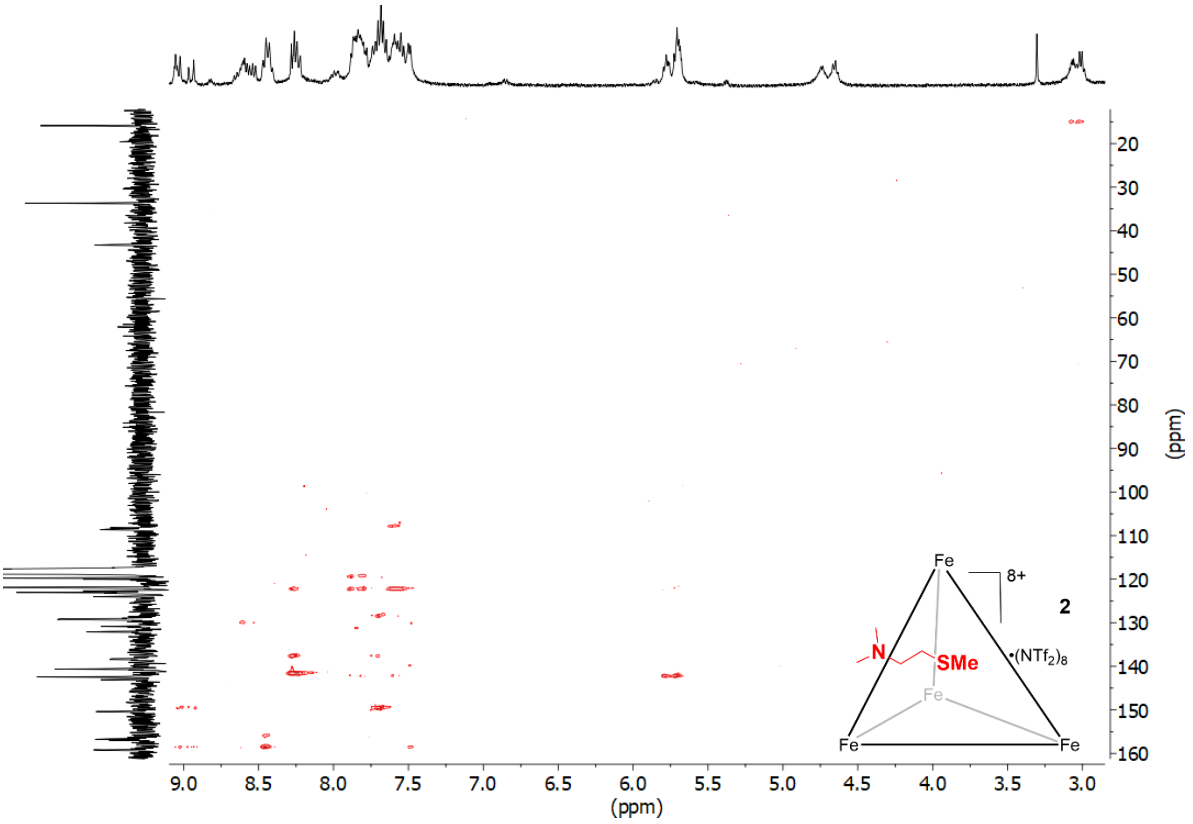

Figure *S-22*. HMBC NMR spectrum of **2** (600 MHz, 298 K, CD_3CN).

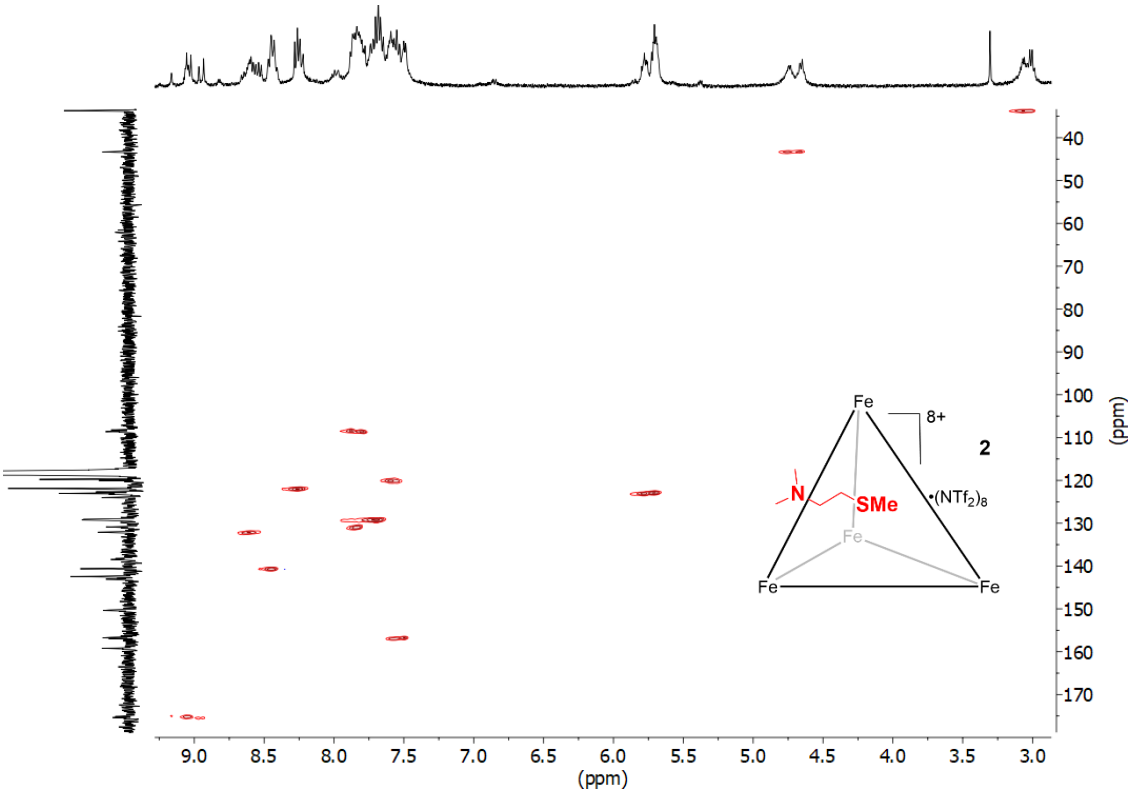

Figure *S-23.* HSQC NMR spectrum of **2** (600 MHz, 298 K, CD_3CN).

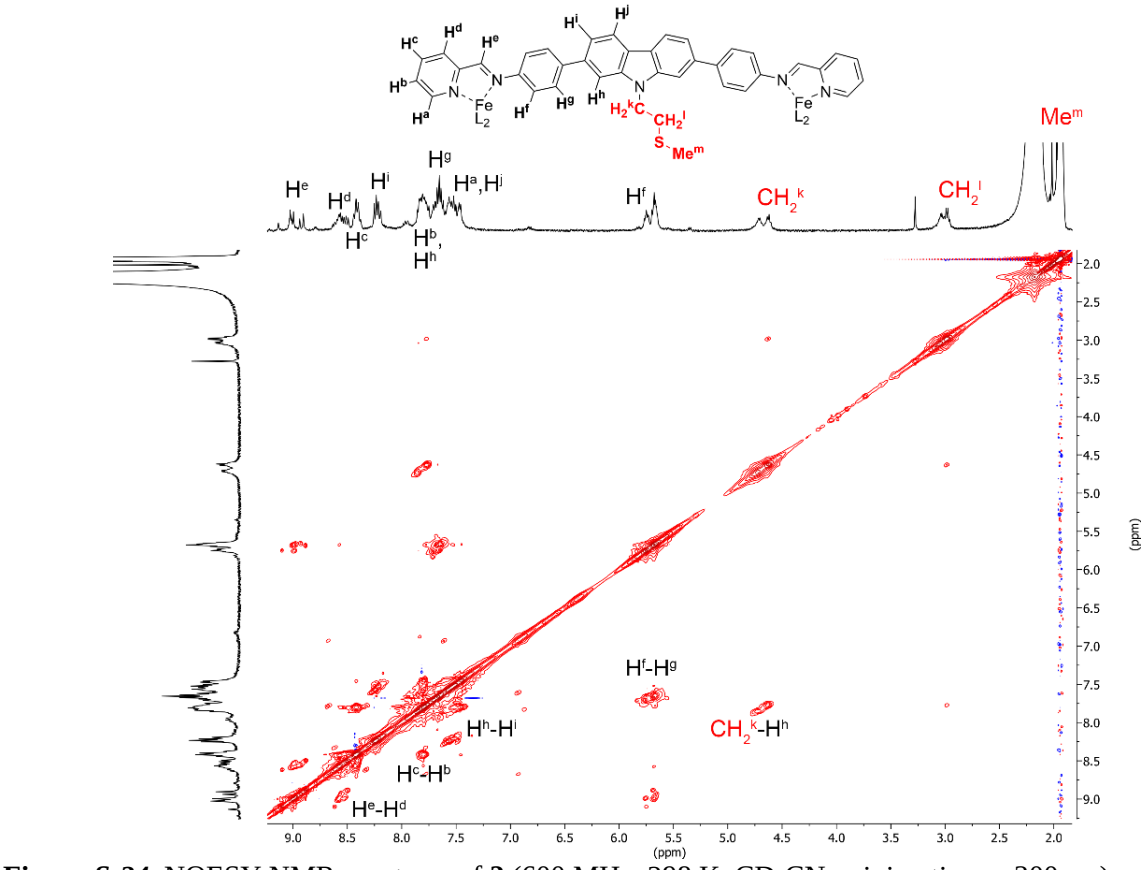

Figure *S-24.* NOESY NMR spectrum of **2** (600 MHz, 298 K, CD_3CN, mixing time = 300 ms).

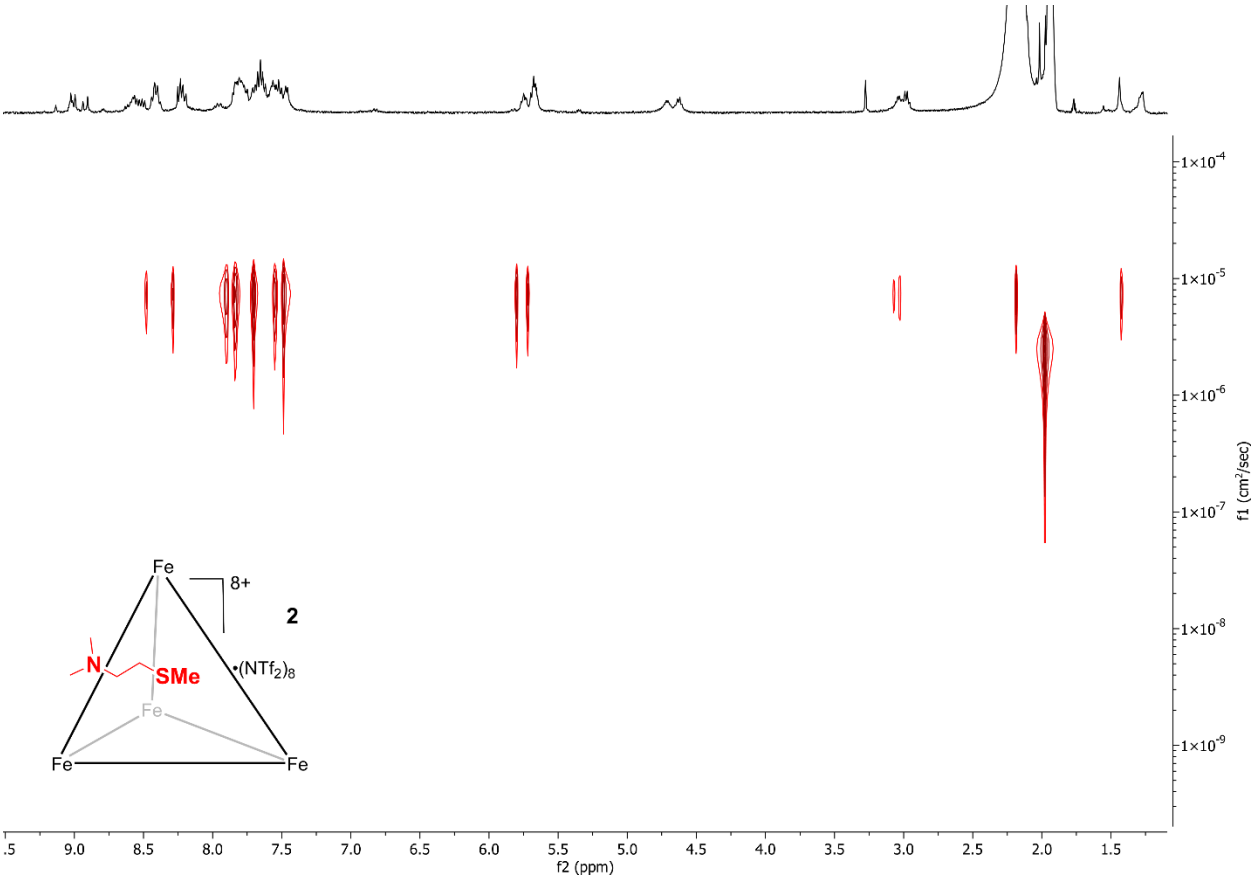

Figure *S-25*. DOSY NMR spectrum of **2** (600 MHz, 298 K, CD_3CN). Diffusion constant; 7.48 x 10^{-6} cm^2/sec.

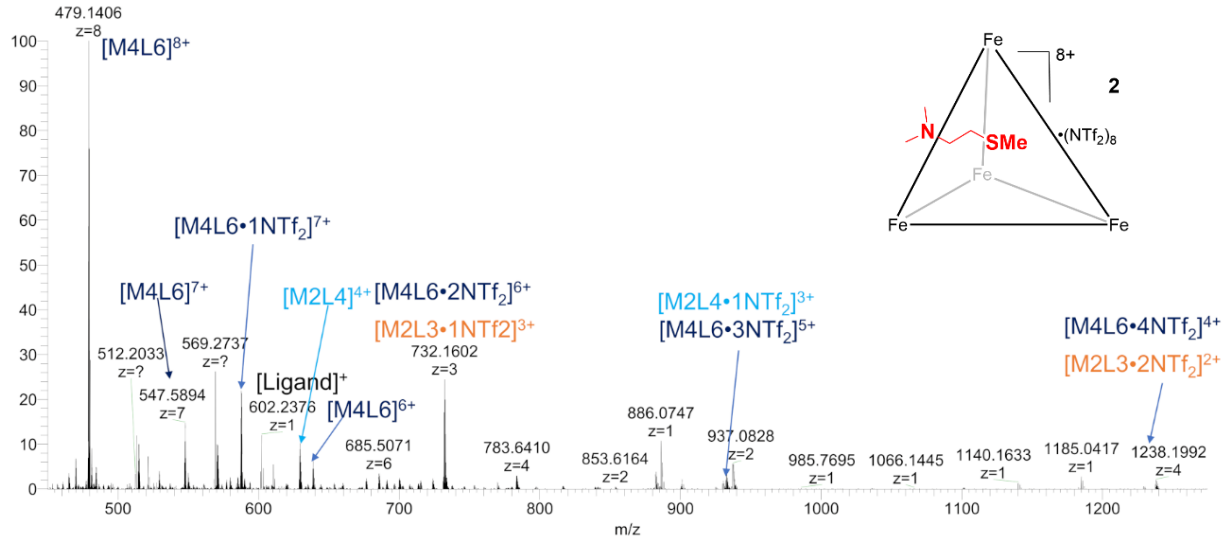

Figure *S-26*. Full mass spectrum of **2** (CH_3CN).

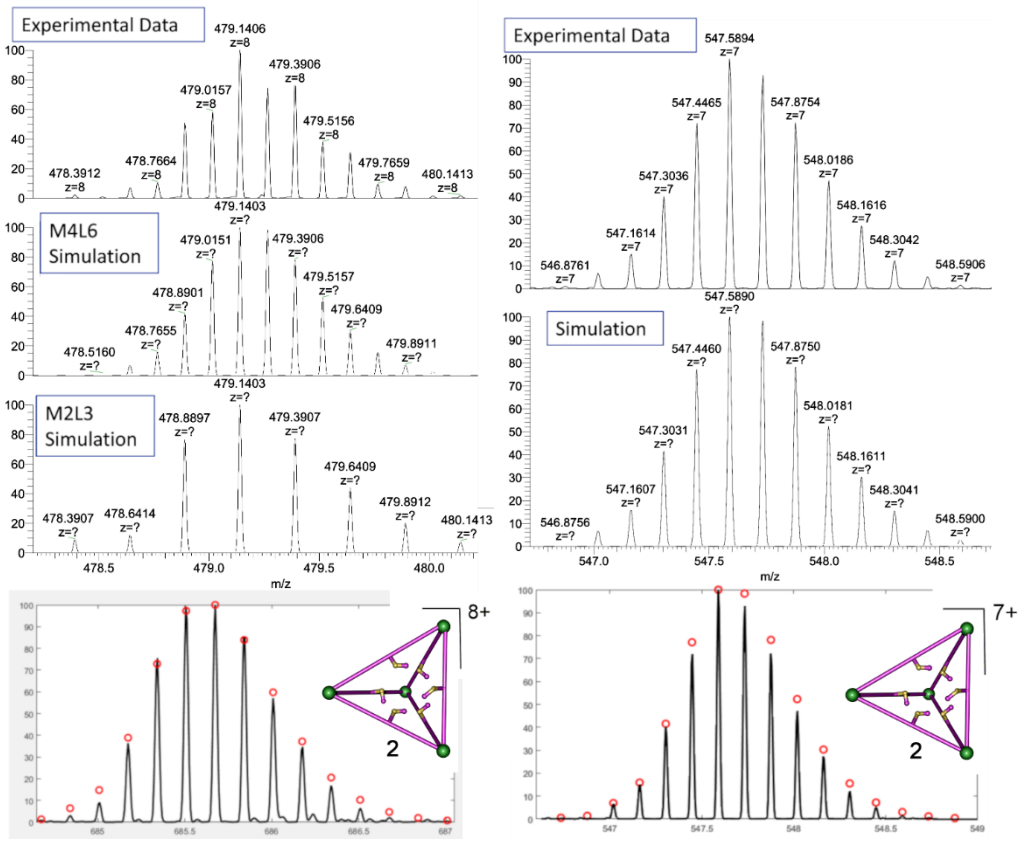

Figure *S-27.* Mass spectra of predicted ions $[\mathbf{2}]^{8+}$ and $[\mathbf{2}]^{7+}$ stacked versus predicted peaks.

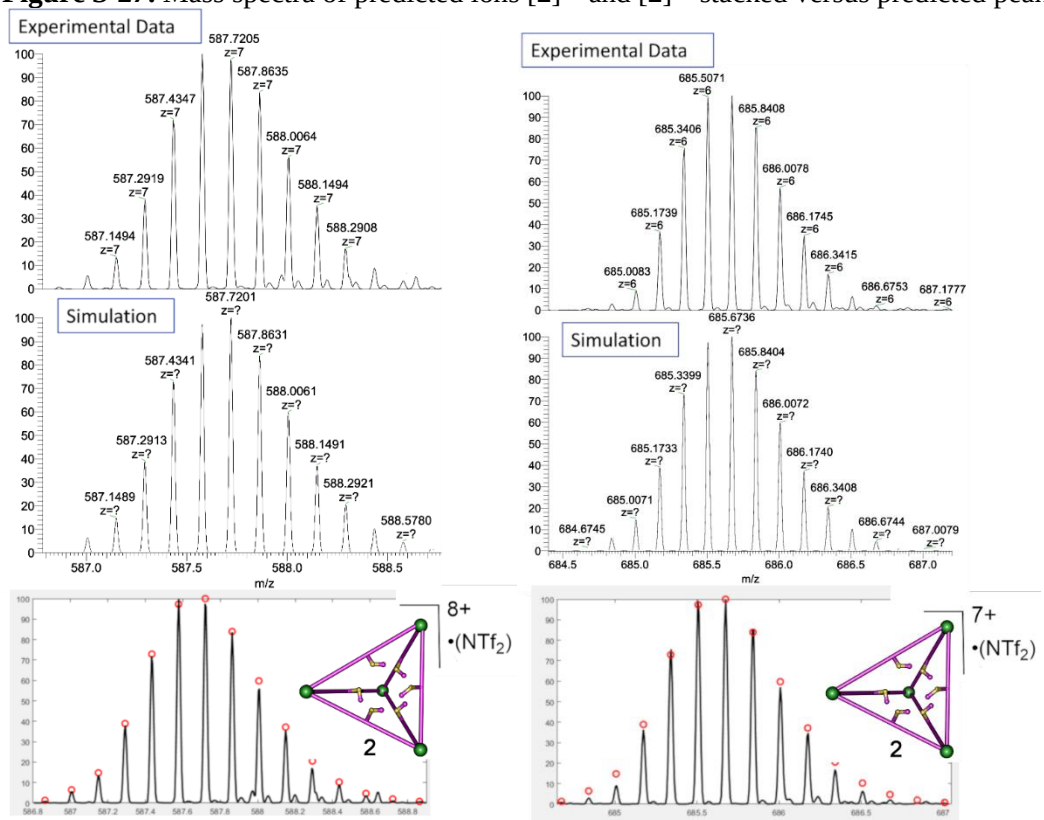

Figure *S-28.* Mass spectra of predicted ions $[\mathbf{2}\bullet 1NTf_2^-]^{7+}$ and $[\mathbf{2}\bullet 1NTf_2^-]^{6+}$stacked versus predicted peaks.

Amine Cage 3:

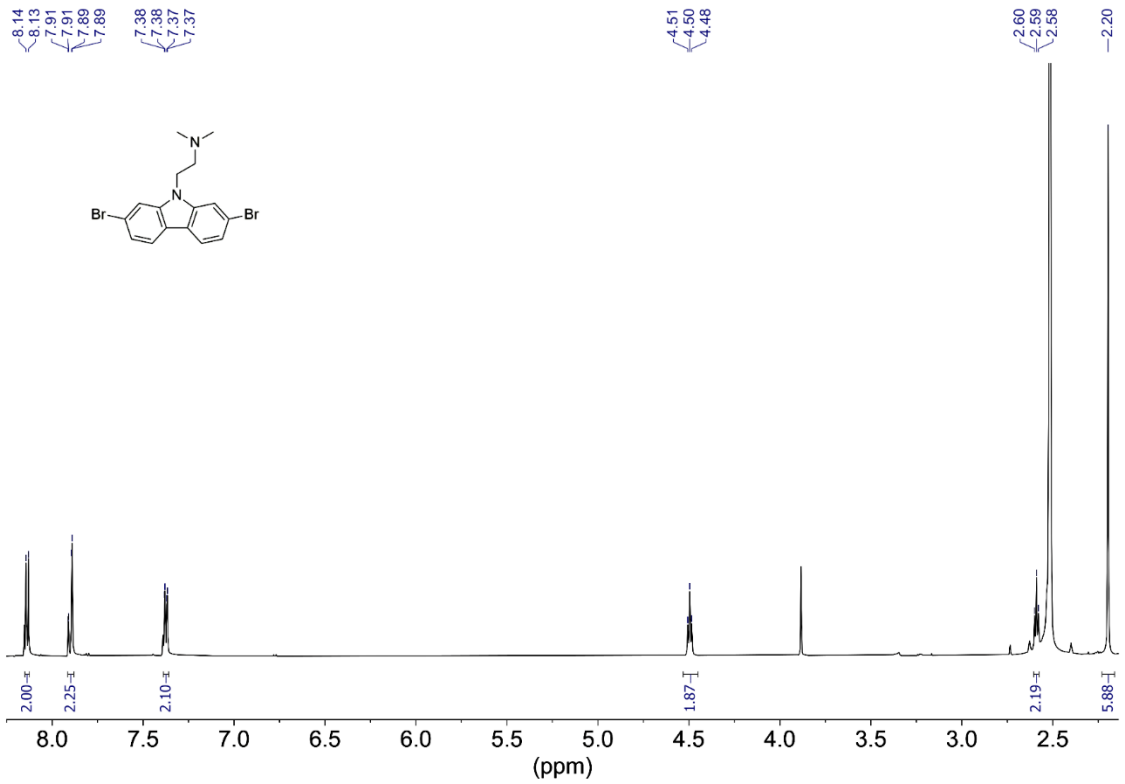

Figure *S-29*. ^{1}H NMR spectrum of **C** (600 MHz, 298 K, DMSO-d_6).

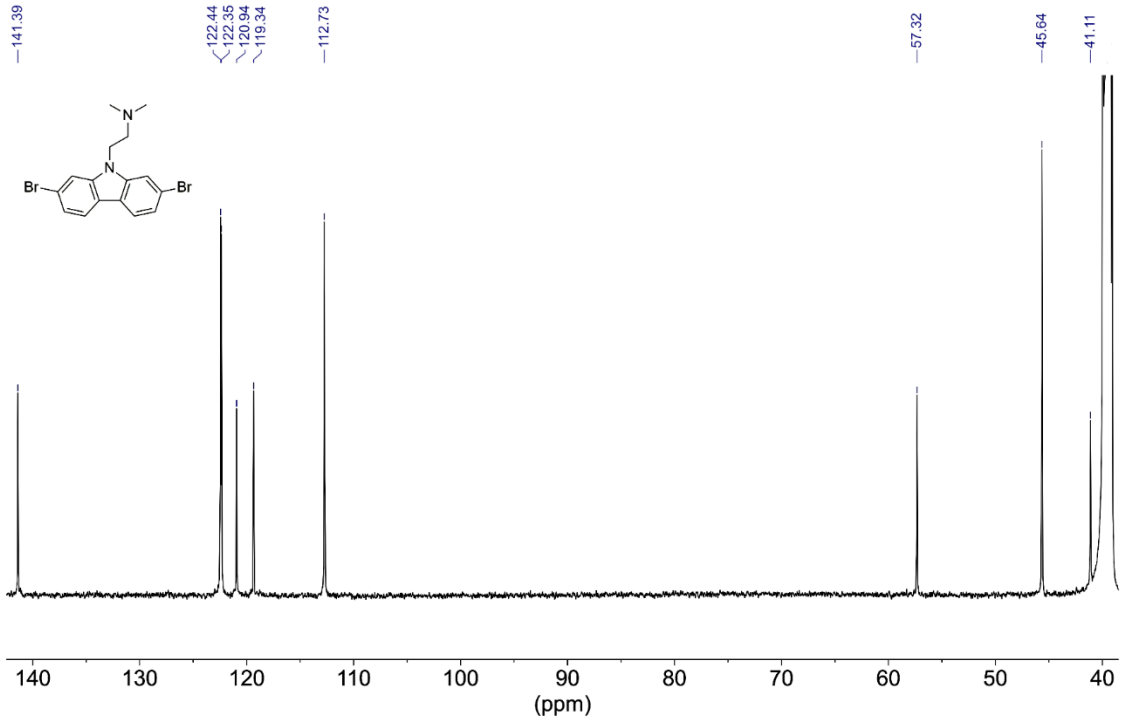

Figure *S-30*. ^{13}C NMR spectrum of **C** (150 MHz, 298 K, DMSO-d_6).

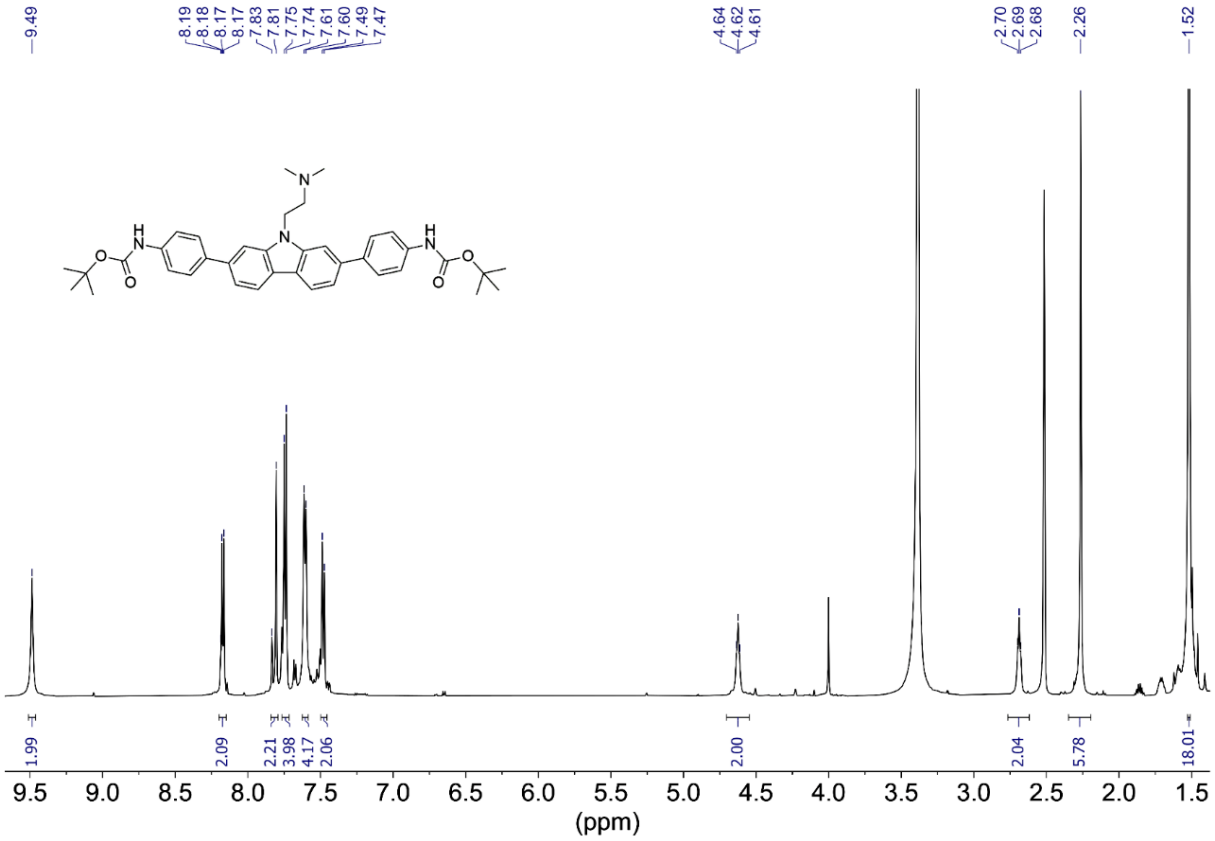

Figure *S-31.* ^{1}H NMR spectrum of ***S*3** (600 MHz, 298 K, DMSO-d_6).

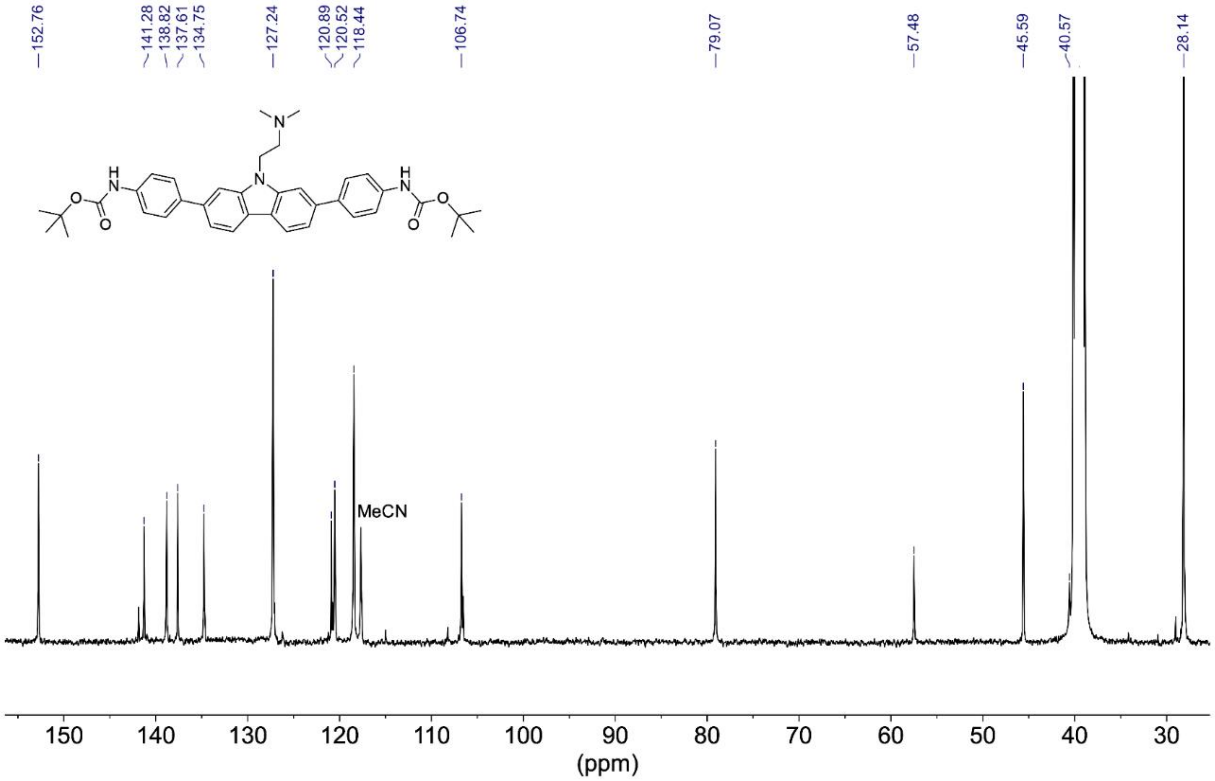

Figure *S-32.* ^{13}C NMR spectrum of ***S*3** (100 MHz, 298 K, DMSO-d_6).

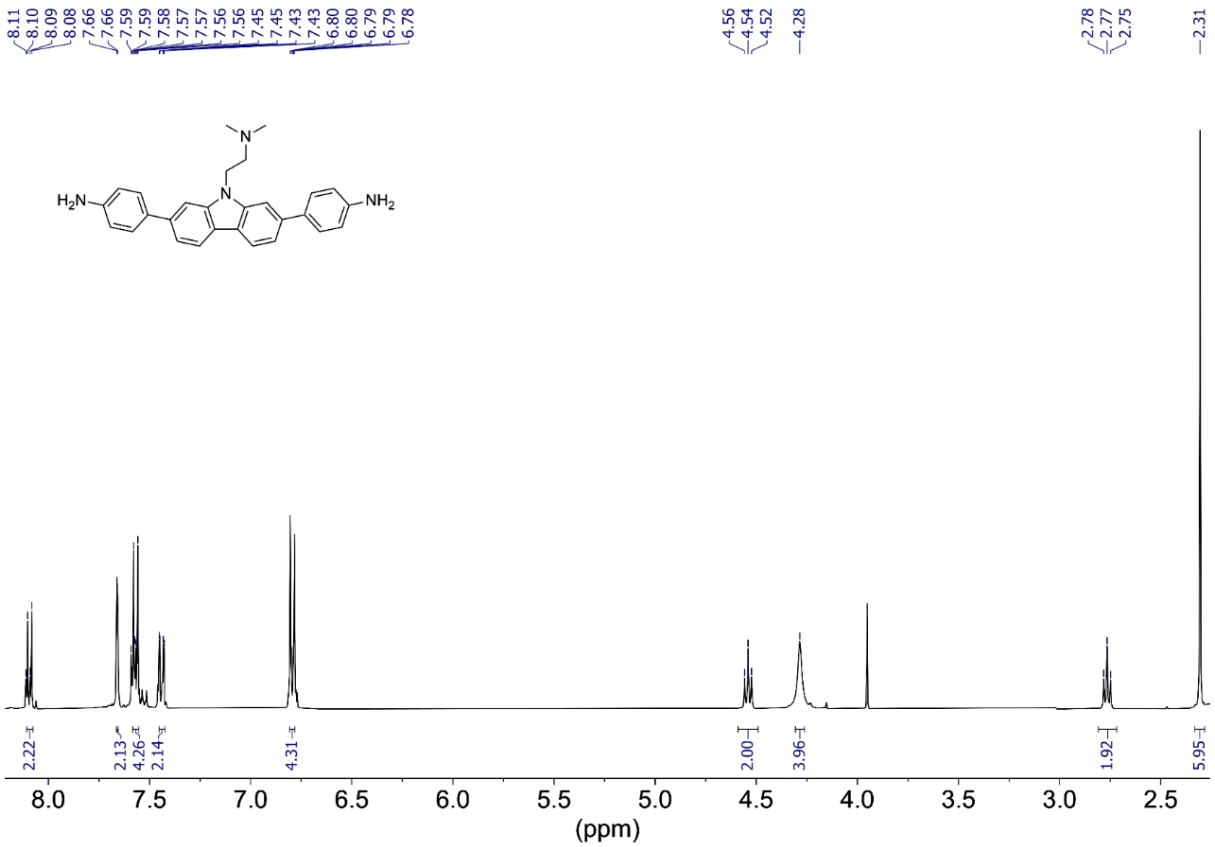

Figure *S-33*. ^{1}H NMR spectrum of **L3** (400 MHz, 298 K, CD_3CN).

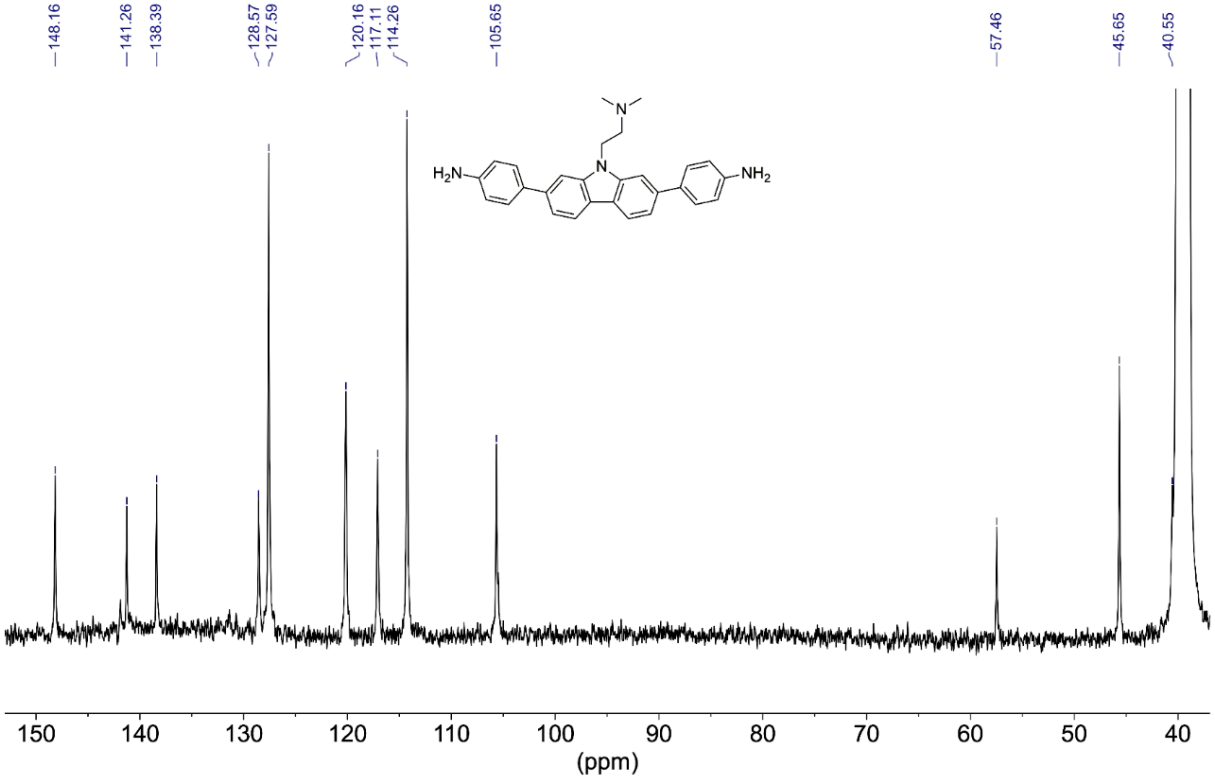

Figure *S-34*. ^{13}C NMR spectrum of **L3** (100 MHz, 298 K, DMSO-d_6).

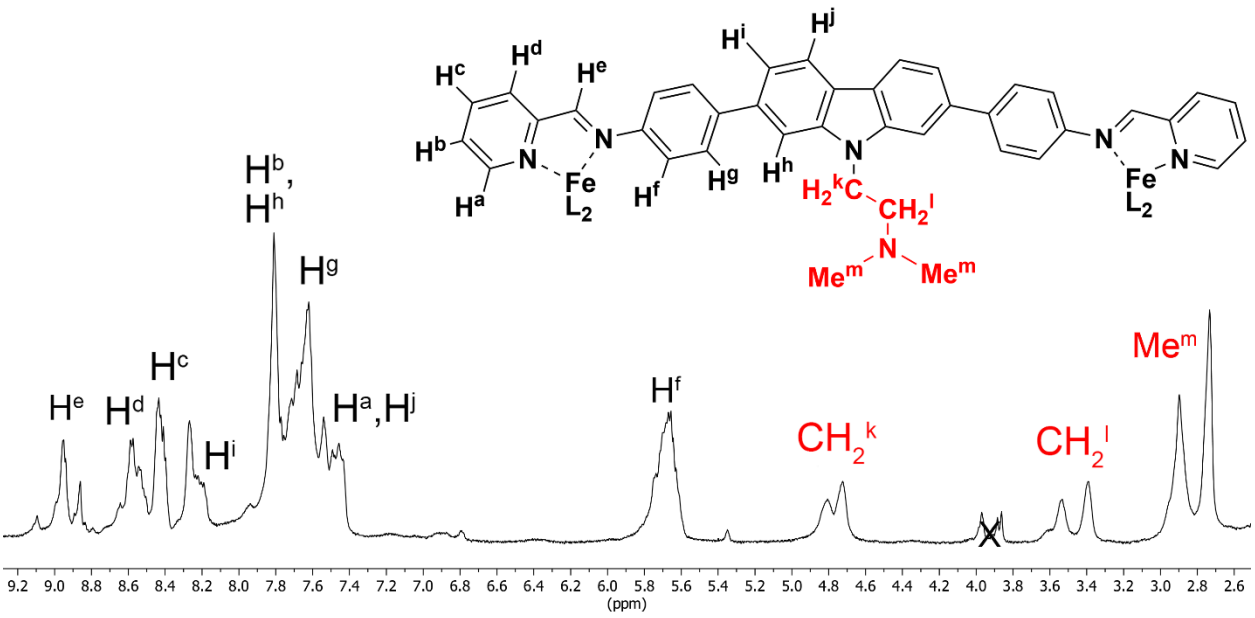

Figure *S-35.* ^{1}H NMR spectrum of **3** (400 MHz, 298 K, CD_3CN).

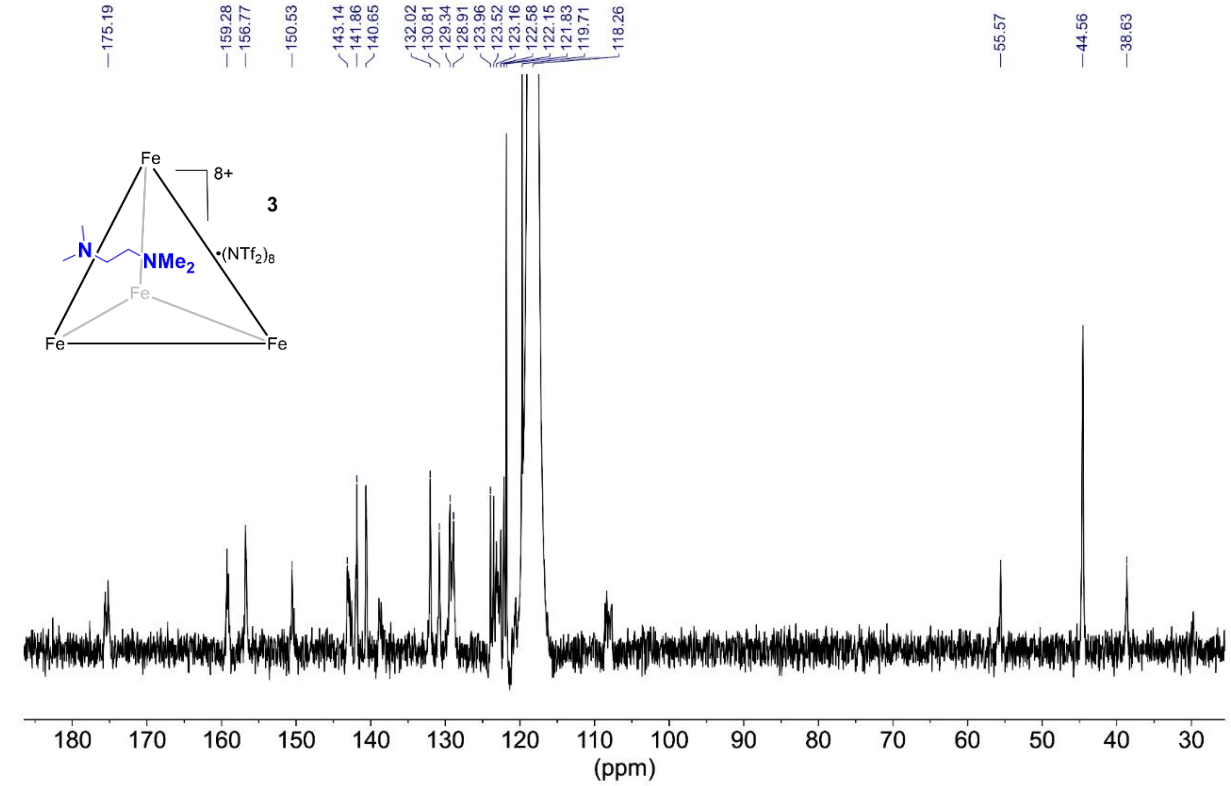

Figure *S-36.* ^{13}C NMR spectrum of **3** (150 MHz, 298 K, CD_3CN).

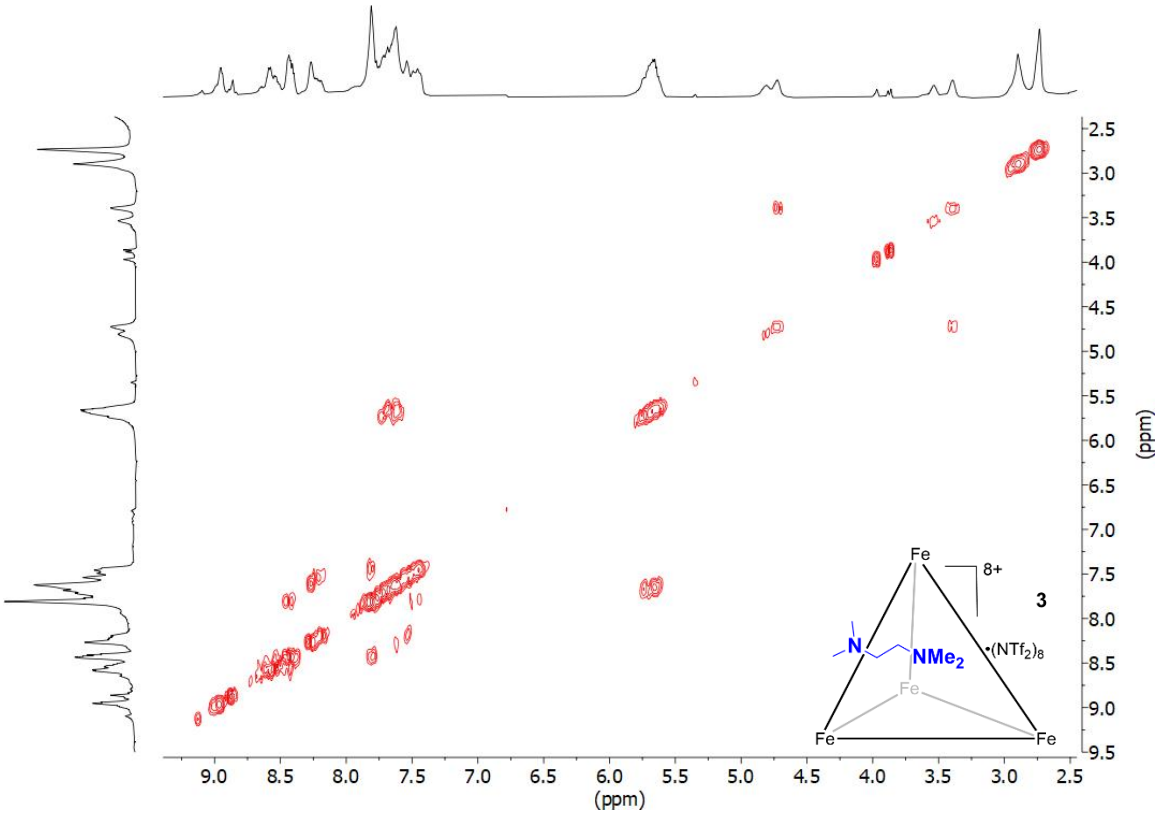

Figure *S-37.* ^{1}H COSY NMR spectrum of **3** (400 MHz, 298 K, CD_3CN).

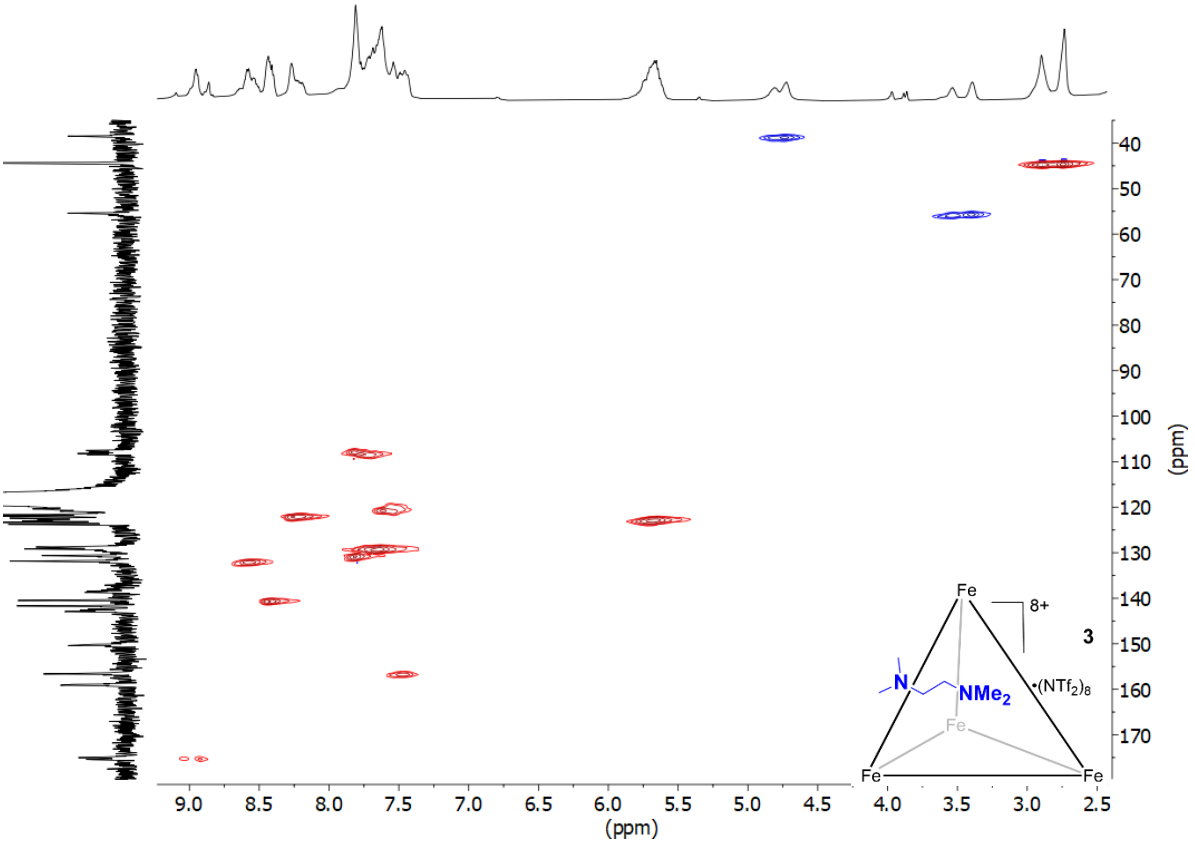

Figure *S-38.* HSQC NMR spectrum of **3** (400 MHz, 298 K, CD_3CN).

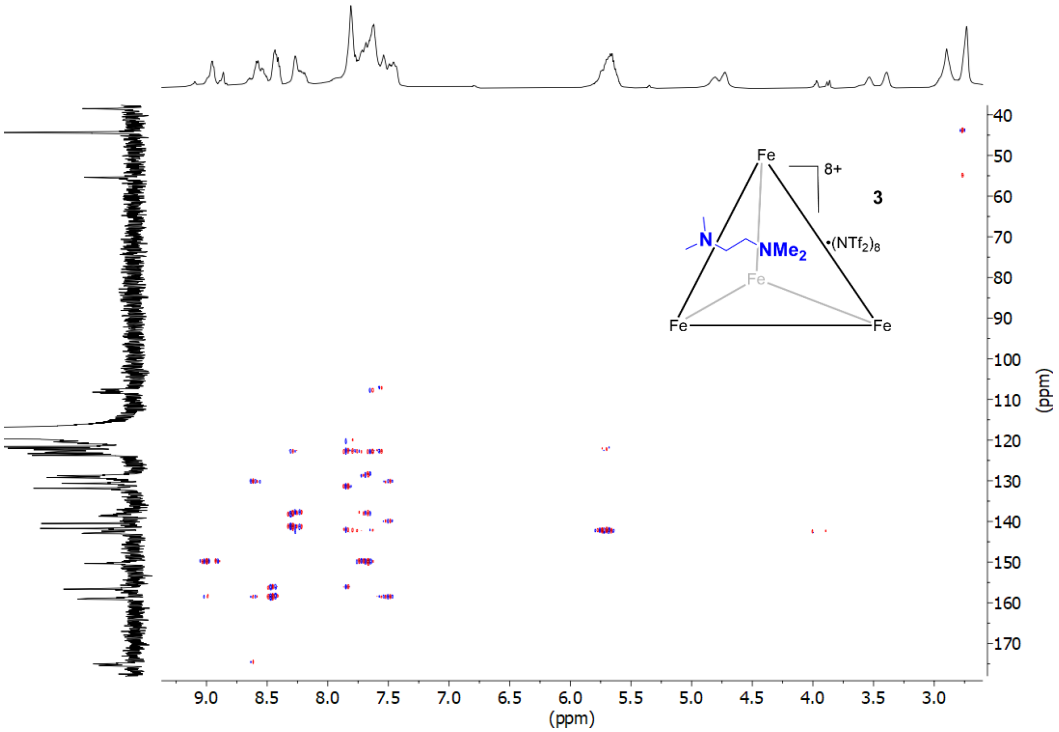

Figure *S-39*. HMBC NMR spectrum of **3** (400 MHz, 298 K, CD_3CN).

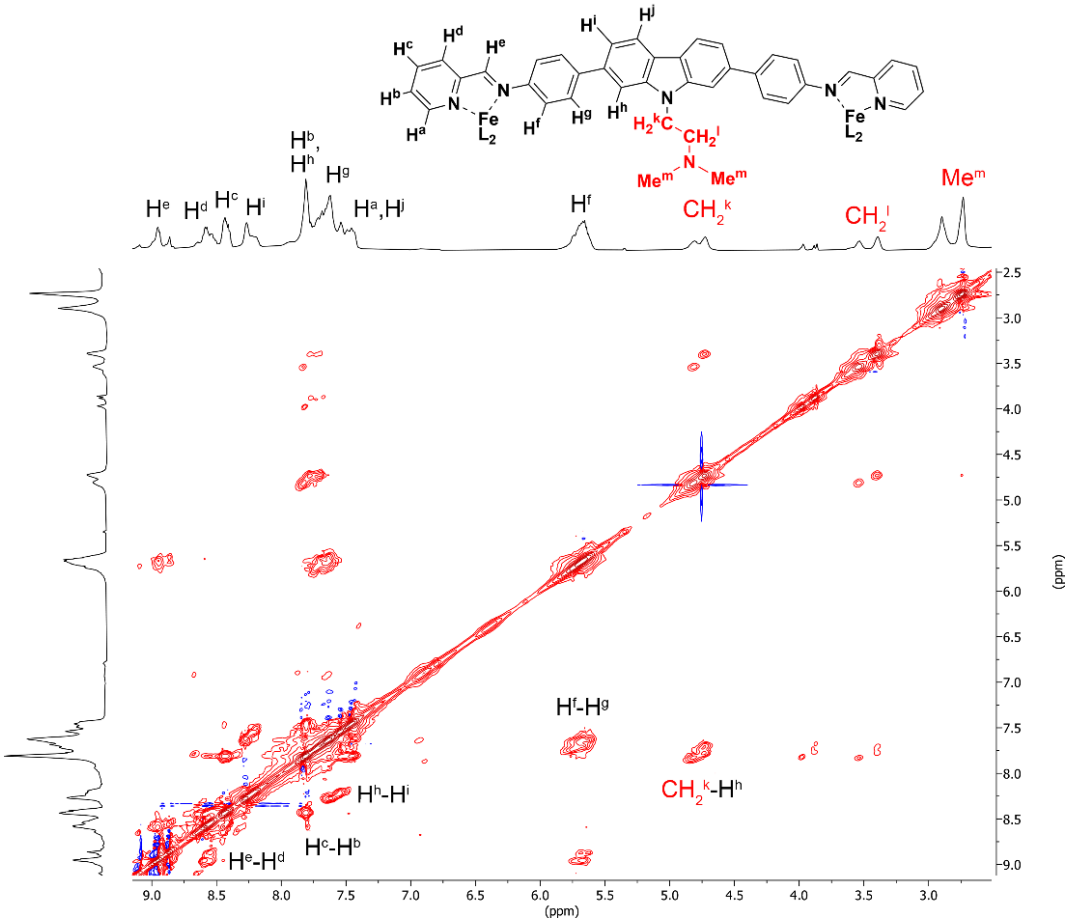

Figure *S-40*. NOESY NMR spectrum of **3** (600 MHz, 298 K, CD_3CN, mixing time = 300 ms).

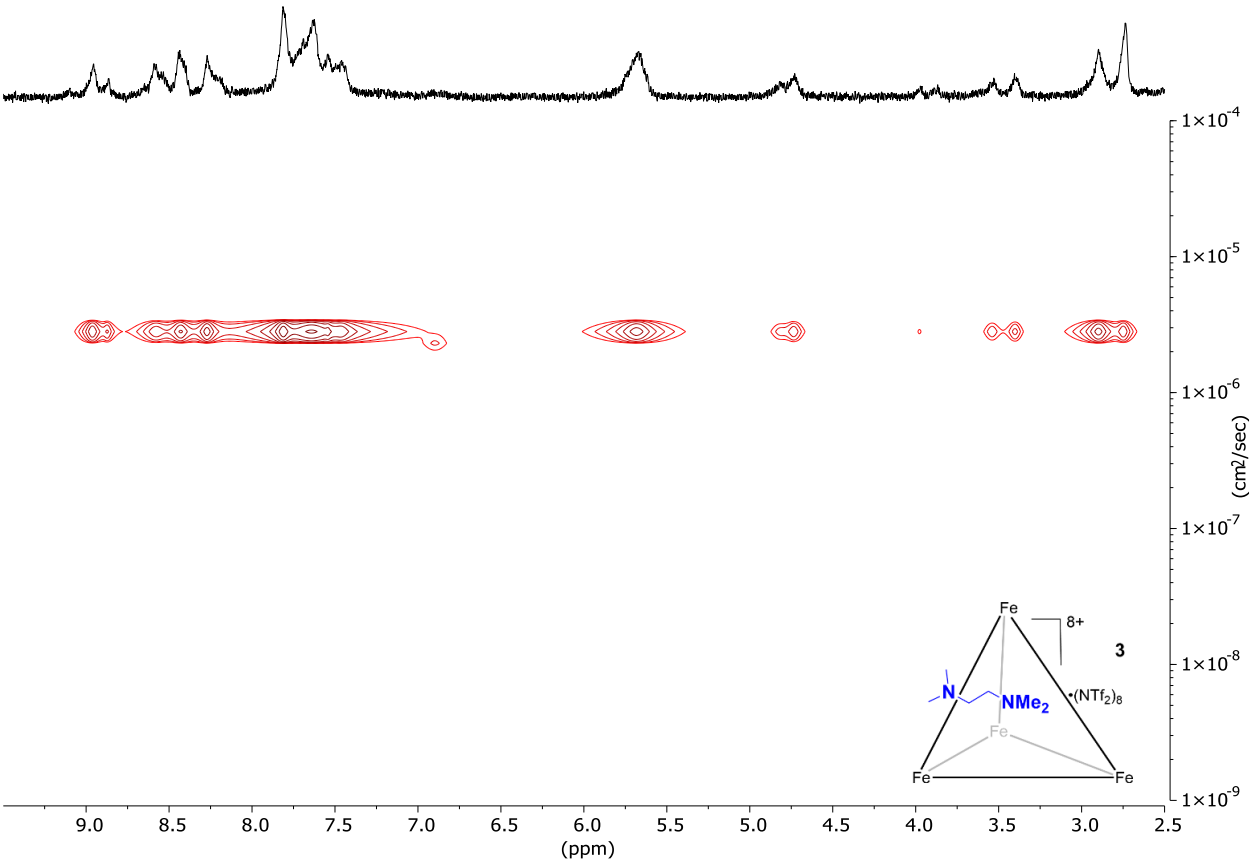

Figure *S-41*. DOSY NMR spectrum of **3** (600 MHz, 298 K, CD_3CN). Diffusion constant; 2.81 x 10^{-6} cm^2/sec.

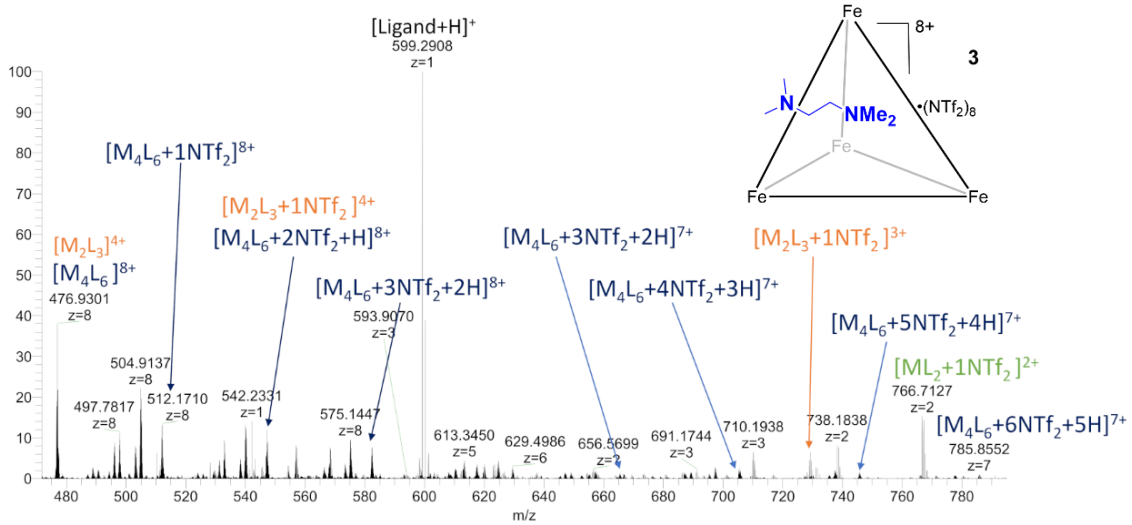

Figure *S-42.* Full mass spectrum of **3** (CH_3CN).

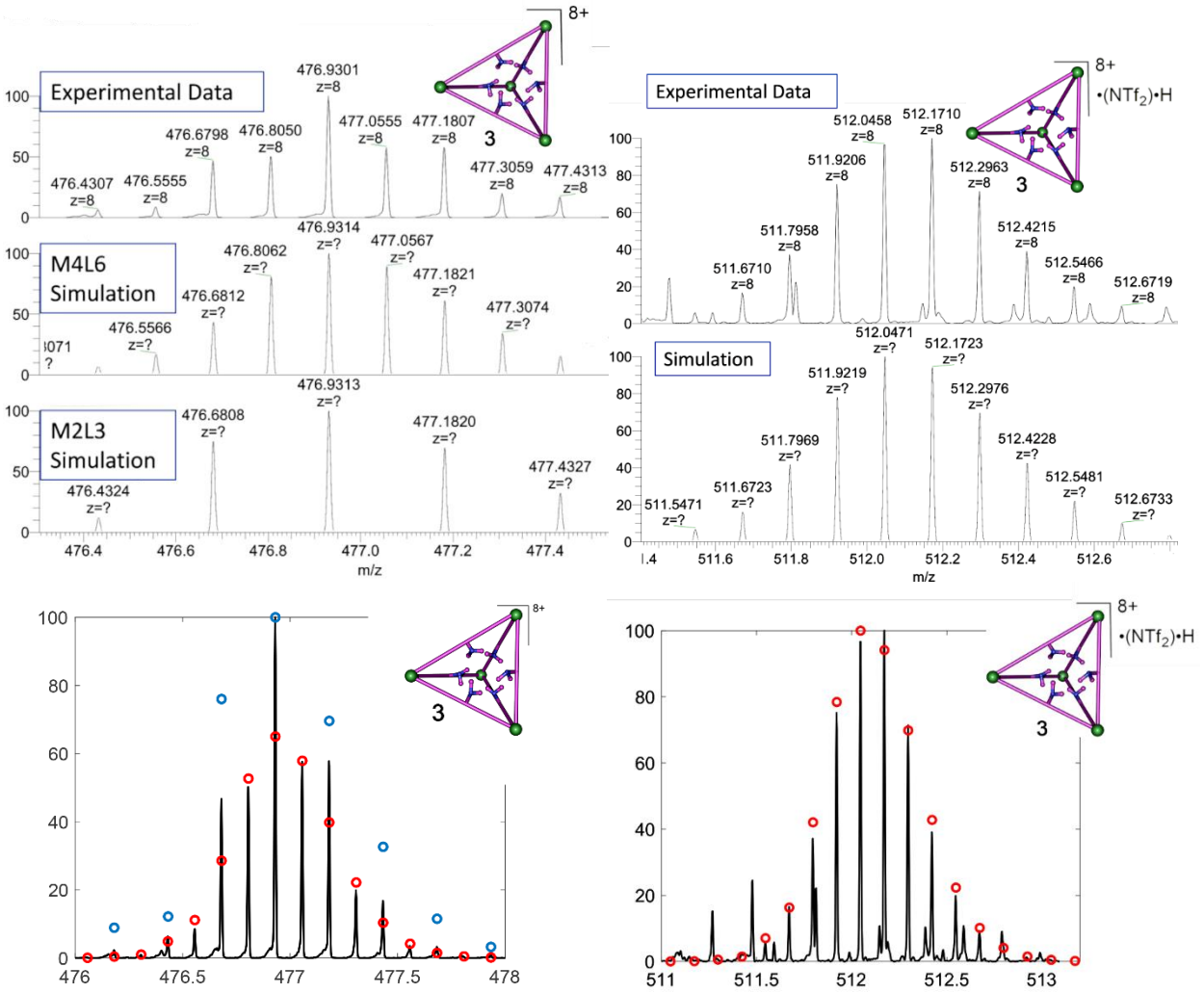

Figure *S-43.* Mass spectra of predicted ions $[\mathbf{3}]^{8+}$ and $[\mathbf{3}\bullet 1NTf_2^- + 1H^+]^{8+}$ stacked versus predicted peaks.

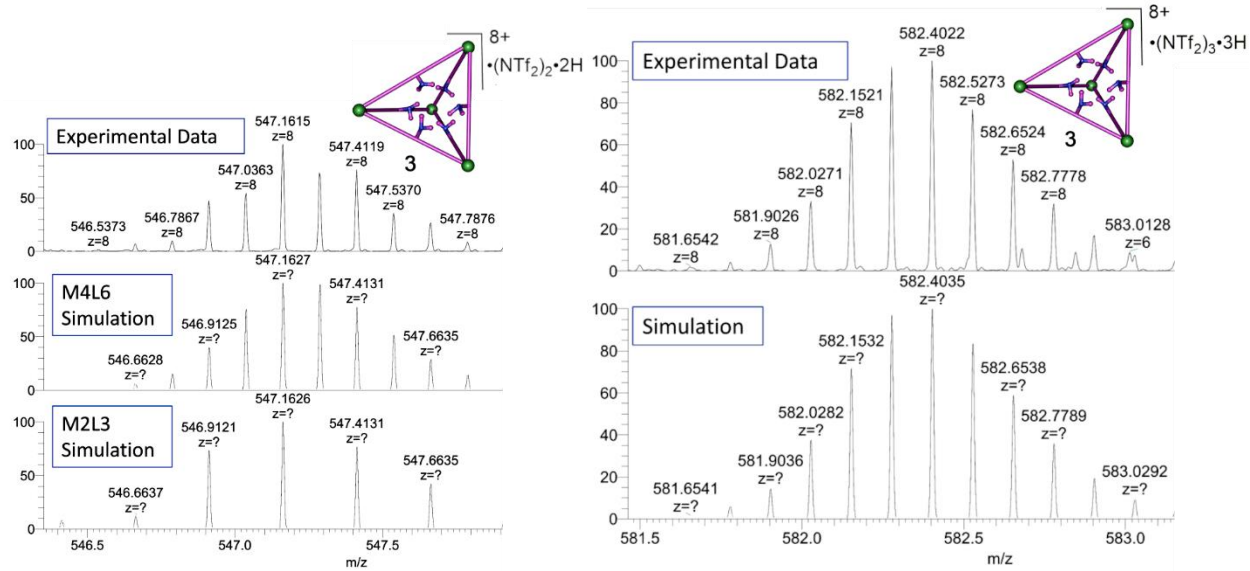

Figure *S-44.* Mass spectra of predicted ions $[\mathbf{3}\bullet 2NTf_2^- + 2H^+]^{8+}$ and $[\mathbf{3}\bullet 3NTf_2^- + 3H^+]^{8+}$ stacked versus predicted peaks.

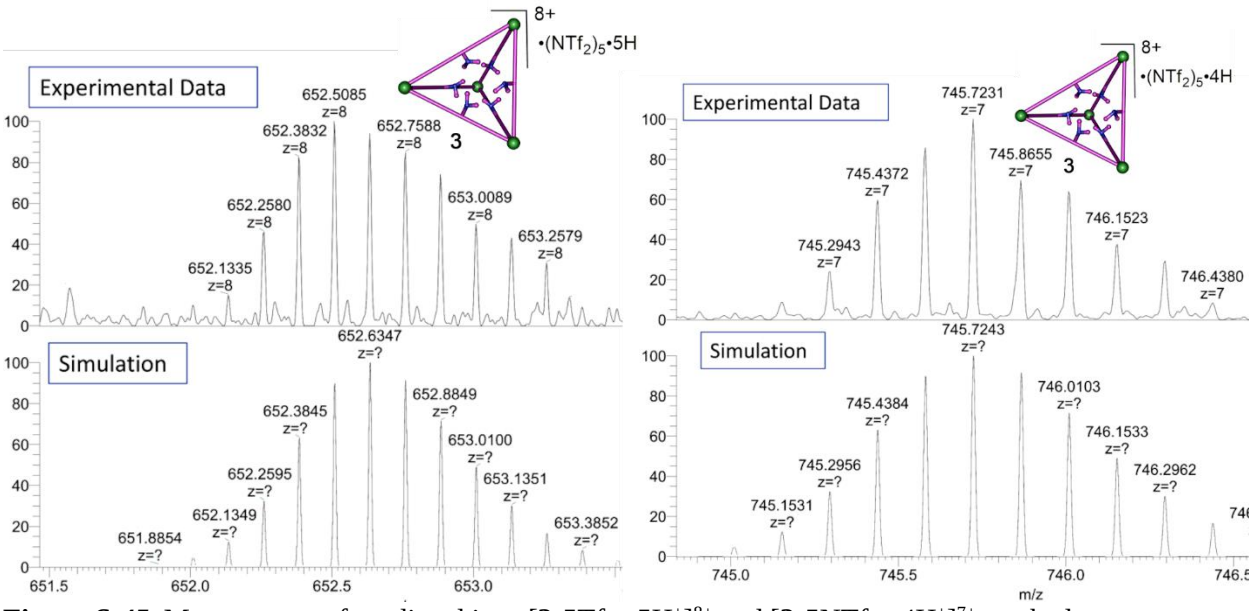

Figure *S-45.* Mass spectra of predicted ions [**3**•5Tf_2^-+5H^+]$^{8+}$ and [**3**•5NTf_2^-+4H^+]$^{7+}$ stacked versus predicted peaks.

II. Photochemistry Data

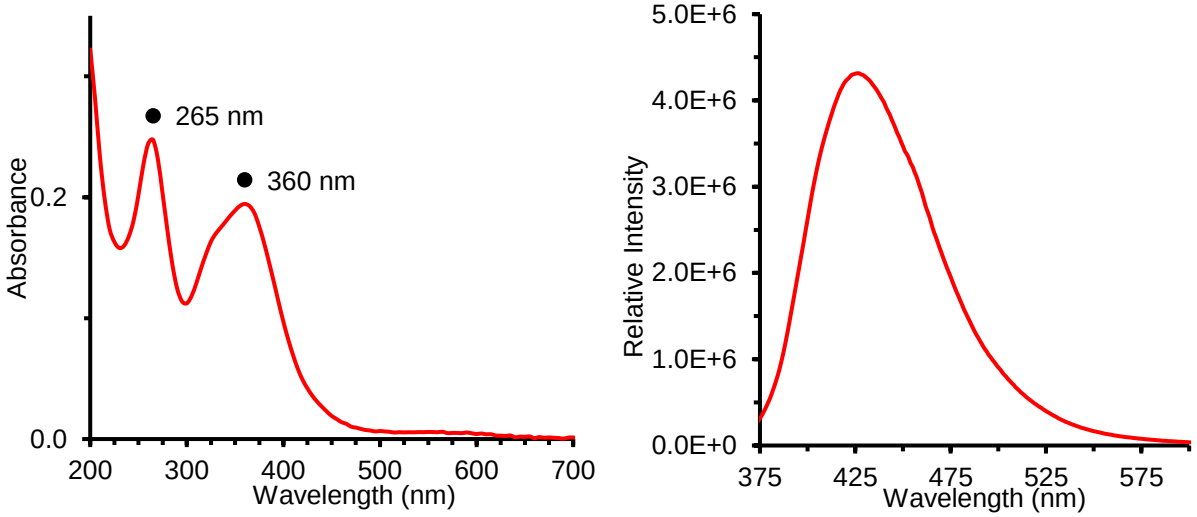

Figure *S-46.* UV-vis absorption spectrum of 1 μM **1** and fluorescence spectrum at 360 nm in CH_3CN.

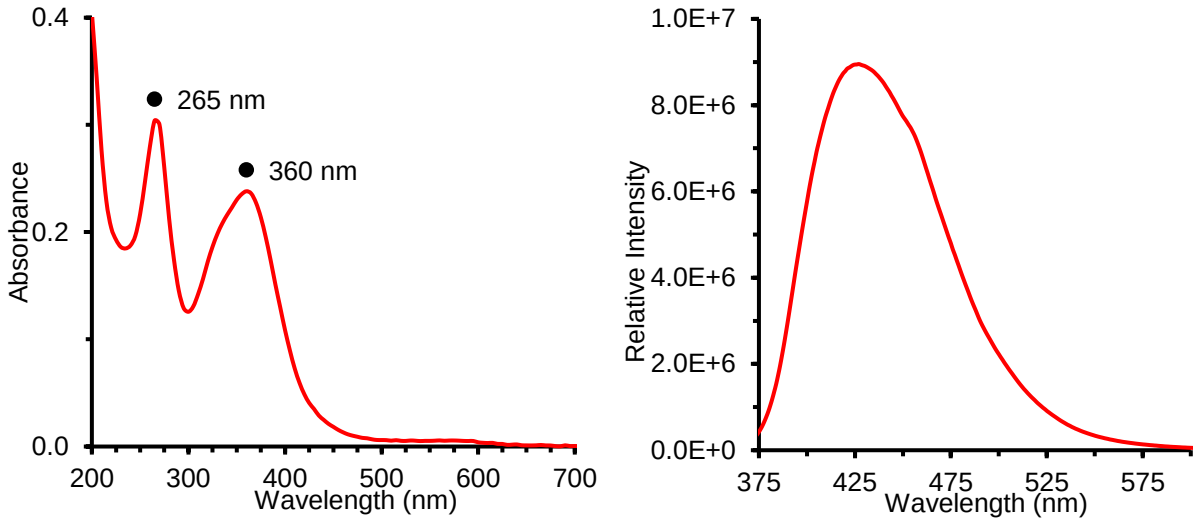

Figure *S-47.* UV-vis absorption spectrum of 1 μM **2** and fluorescence spectrum at 340 nm in CH_3CN.

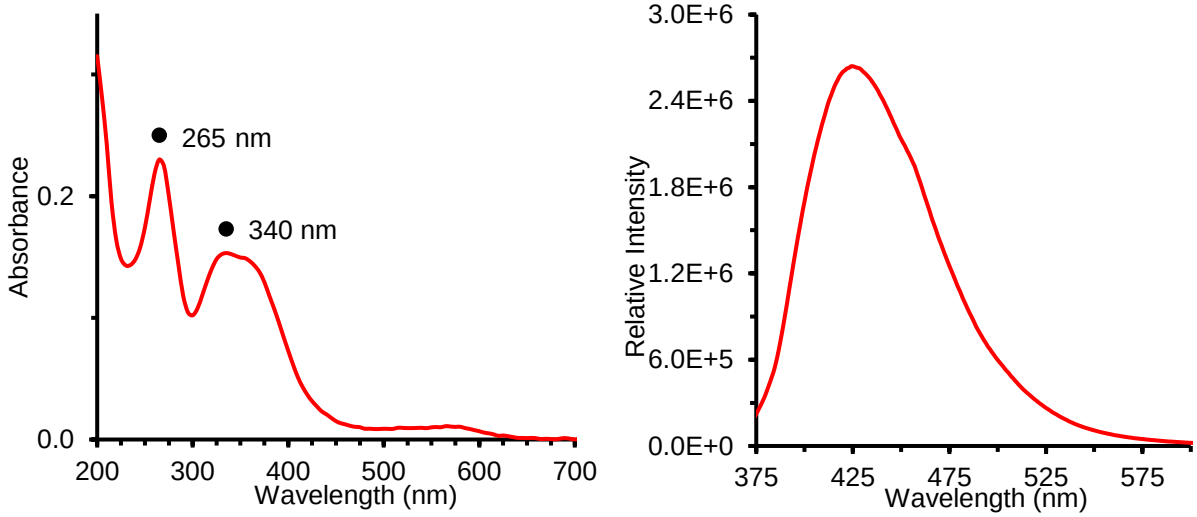

Figure *S-48.* UV-vis absorption spectrum of 1 μM **3** and fluorescence spectrum at 340 nm in CH_3CN.

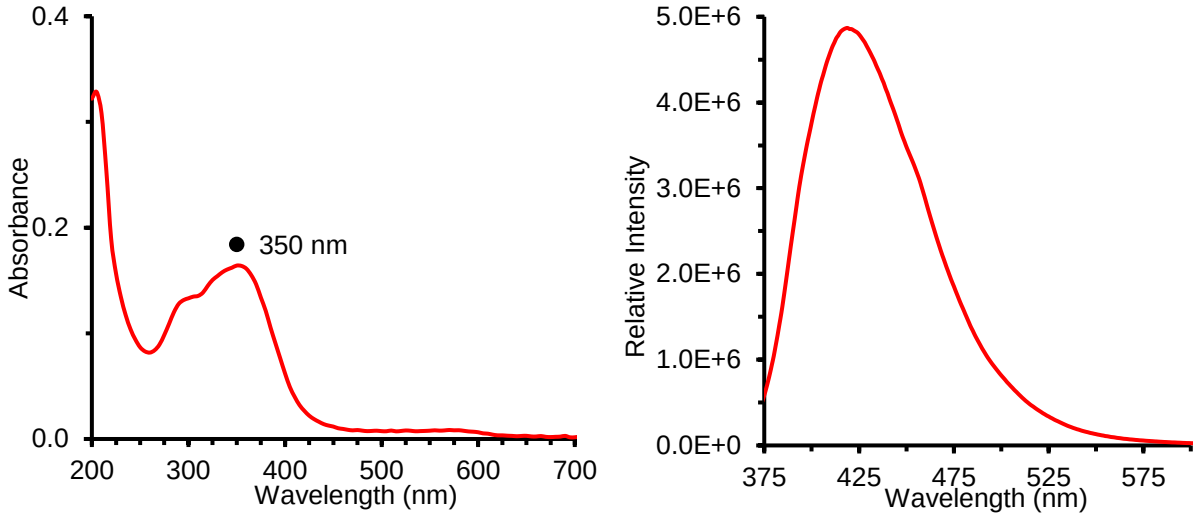

Figure *S-49*. UV-vis absorption spectrum of 1 μM **4** and fluorescence spectrum at 350 nm in CH_3CN.

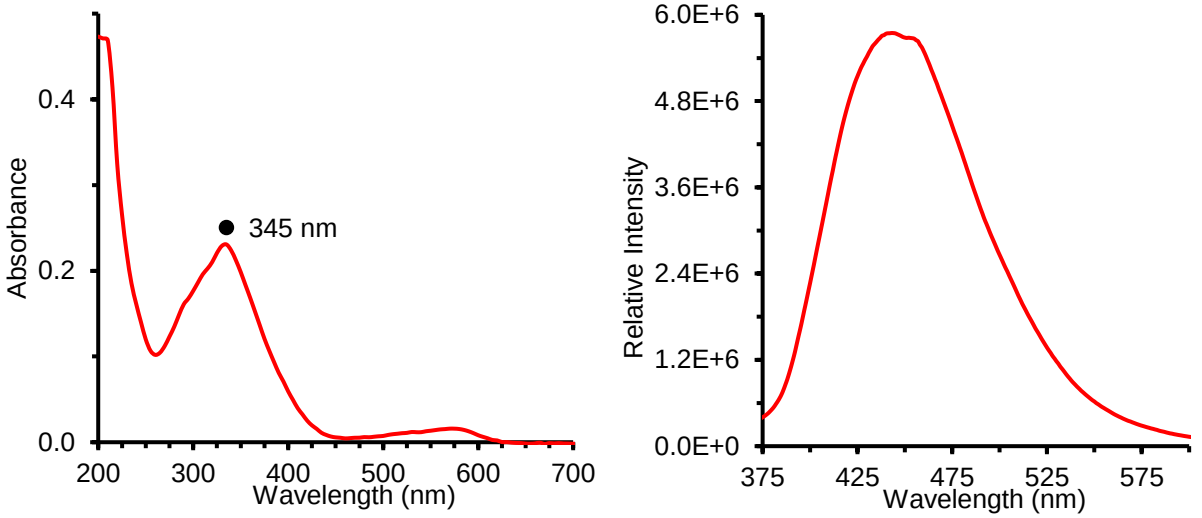

Figure *S-50*. UV-vis absorption spectrum of 1 μM **5** and fluorescence spectrum at 333 nm in CH_3CN.

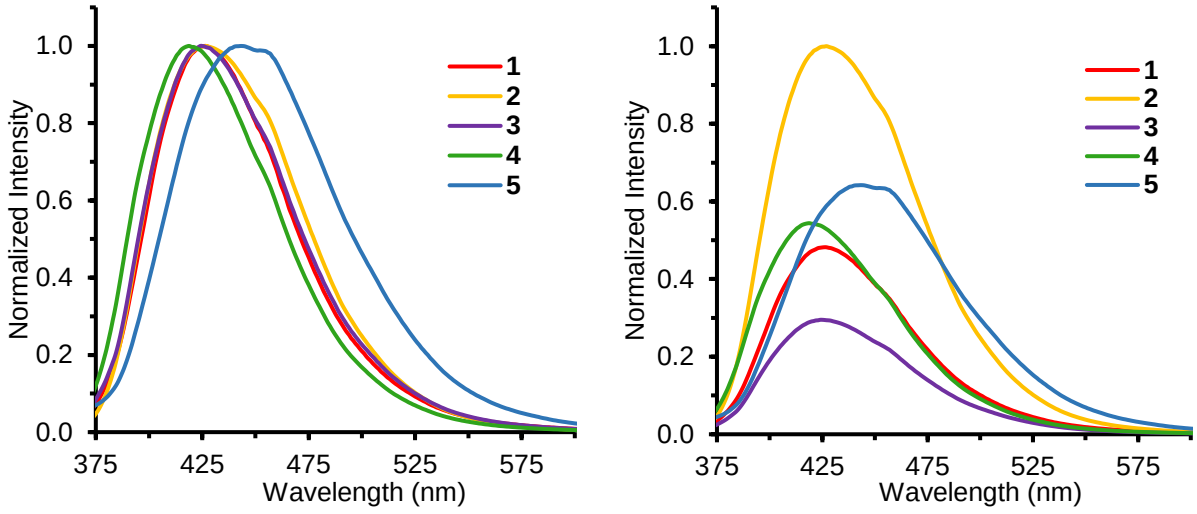

Figure *S-51*. Fluorescence spectra of cages **1-5** relative to max emissions and normalized emissions.

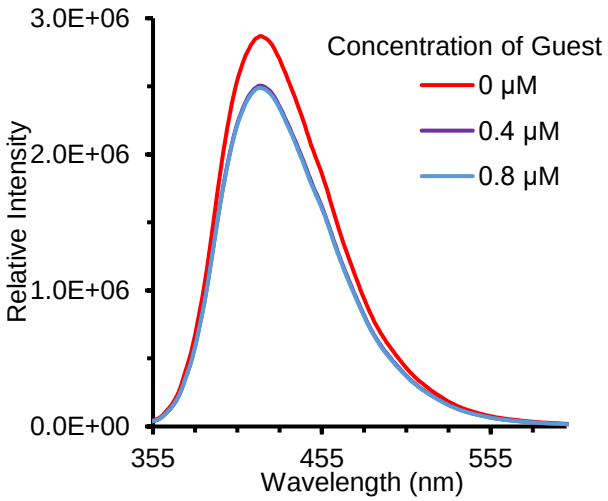

Figure *S-52*. Fluorescence spectra of the titration of DABCO into a 0.2 μM solution of cage **3** in CH_3CN. DABCO was added in 0.4 μL aliquots from a 3 mM stock solution in CH_3CN.

III. Binding Studies

Table *S-1:* Binding affinities of guests **6-14** in cages **1-3**,[a] including binding results from fitting to a 1:1 and 1:2 algorithm in each case. Entries in red were deemed "poor fits" and not shown in Table 1 (main text) due to excessive fitting errors.

Guest	Cage 1		Cage 2		Cage 3	
	K_a(1:1), x 10^3 M^{-1}	K_{11}, K_{12} (1:2), x 10^3 M^{-1}	K_a(1:1), x 10^3 M^{-1}	K_{11}, K_{12}(1:2), x 10^3 M^{-1}	K_a(1:1), x 10^3 M^{-1}	K_{11}, K_{12} (1:2), x 10^3 M^{-1}
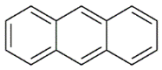 **6**	120 ± 6.8	K_{11}: 89 ± 2.8 K_{12}: 1.7 ± 0.1	110 ± 5.9	K_{11}: 51 ± 2.1 K_{12}: 64 ± 13	99 ± 5.7	K_{11}: 110 ± 7.7 K_{12}: 2.0 ± 0.4
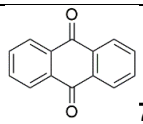 **7**	100 ± 5.5	K_{11}: 210 ± 8.8 K_{12}: 23 ± 0.6	80 ± 3.8	K_{11}: 1800 ± 1300 K_{12}: 54 ± 3.0	110 ± 4.2	K_{11}: 88 ± 5.6 K_{12}: 37 ± 18
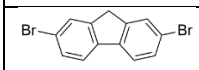 **8**	74 x ± 3.6	K_{11}: 160 ± 13 K_{12}: 2.1 ± 0.2	83 ± 3.6	K_{11}: 130 ± 11 K_{12}: 0.5 ± 0.08	58 ± 2.4	K_{11}: 64 ± 3.2 K_{12}: 6.8 ± 1.1
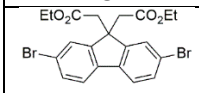 **9**	160 ± 11	K_{11}: 650 ± 220 K_{12}: 110 ± 9.9	61 ± 1.2	K_{11}: 430 ± 29 K_{12}: 100 ± 3.9	70 ± 2.5	K_{11}: 120 ± 4.8 K_{12}: 0.7 ± 0.04
n-octylSH **10**	320 ± 28	K_{11}: 5800 ± 1600 K_{12}: 2.8 ± 0.2	140 ± 14	K_{11}: 12000 ± 8300 K_{12}: -39 ± -2.3	230 ± 18	K_{11}: 56000 ± 190000 K_{12}: 90 ± 12
adamantanone **11**	1600 ± 290	K_{11}: 250000 ± 420000 K_{12}: 210 ± 15	720 ± 74	K_{11}: 6600 ± 1700 K_{12}: 300 ± 17	440 ± 26	K_{11}: 1500 ± 230 K_{12}: 89 ± 6.8
adamantanol **12**	1800 ± 360	K_{11}: 63000 ± 75000 K_{12}: 150 ± 19	540 ± 64	K_{11}: 260000 ± 620000 K_{12}: 161 ± 8.1	490 ± 27	K_{11}: 680 ± 37 K_{12}: 120 ± 7.6
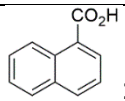 **13**	18 ± 0.7	K_{11}: 26 ± 0.8 K_{12}: 370 ± 27	77 ± 3.2	K_{11}: 300 ± 41 K_{12}: 59 ± 2.7	86 ± 5.2	K_{11}: 76 ± 4.0 K_{12}: 0.5 ± 0.05
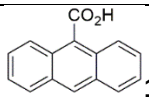 **14**	120 ± 9.2	K_{11}: 49 ± 2.7 K_{12}: 4.8 ± 0.4	100 ± 9.1	K_{11}: 18 ± 8.2 K_{12}: 910 ± 450	79 ± 3.8	K_{11}: 440 ± 160 K_{12}: 90 ± 6.3

[a]in CH_3CN, [**1-3**] = 1.0 μM, absorbance changes measured at 325 nm and 365 nm, affinities calculated via the Nelder-Mead method.[1-3]

UV/Vis Titrations of Guests into cage 1:

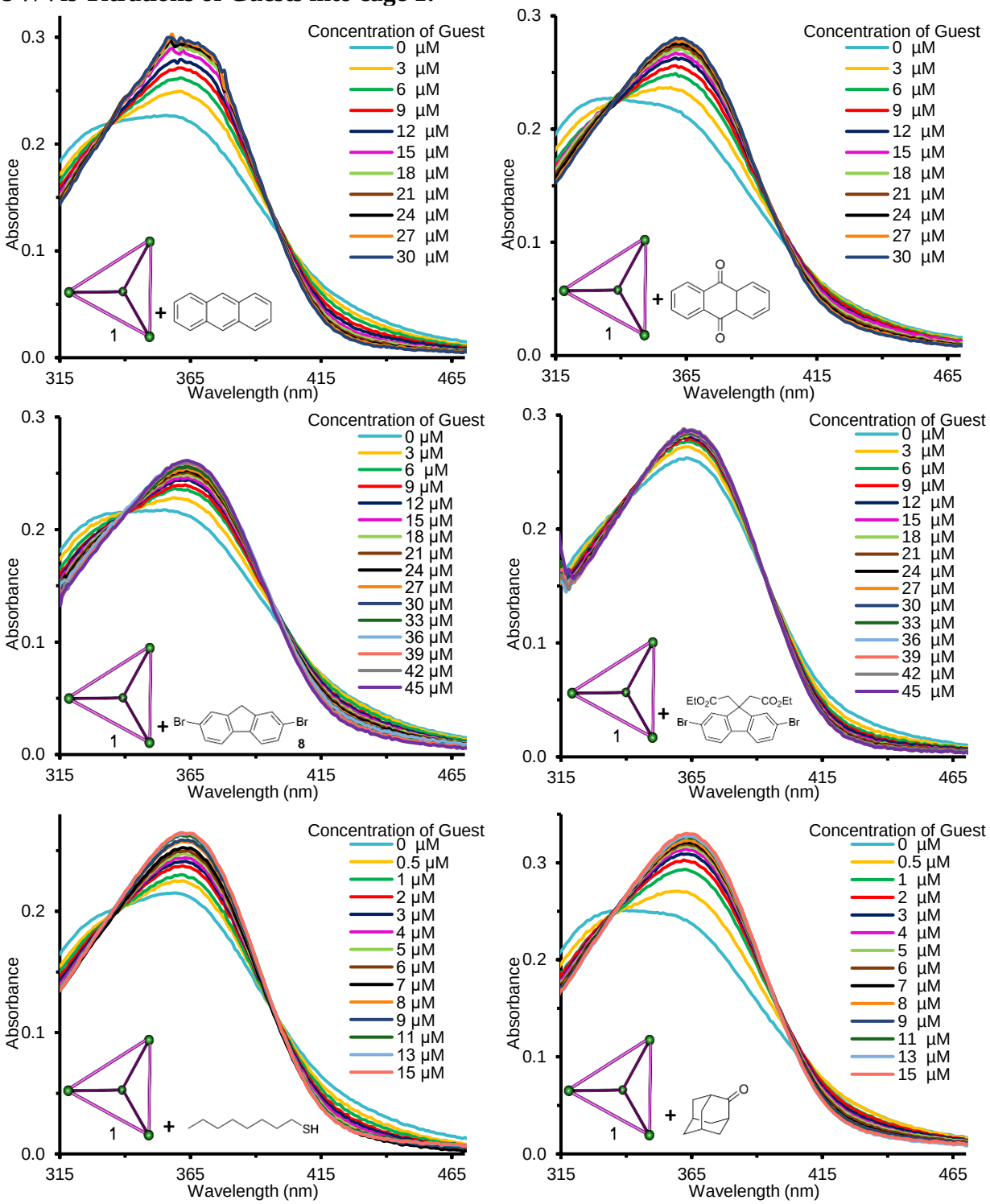

Figure *S-53.* UV-Vis absorption spectra of the titrations of guests **6–11** into 1 µM solutions of cage **1** in CH_3CN. Guests were added in 0.5 or 1 µL aliquots from 3 or 9 mM stock solutions in CH_3CN.

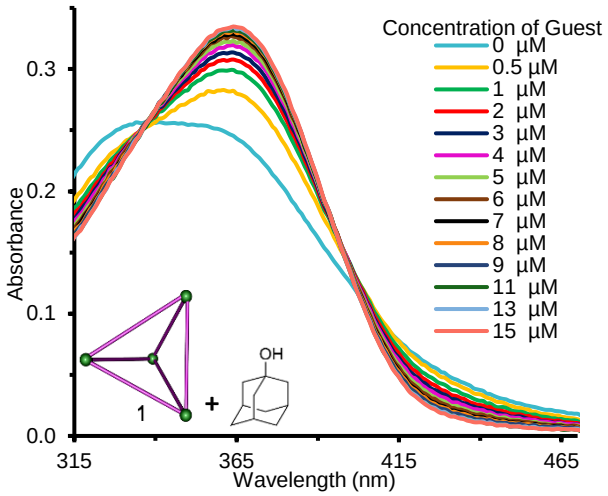

Figure *S-54.* UV-Vis absorption spectrum of the titration of **12** into 1 µM solutions of cage 1 in CH_3CN. Guest was added in 0.5 and 1 µL aliquots from a 3 mM stock solution in CH_3CN.

UV/Vis Titrations of Guests into cage 2:

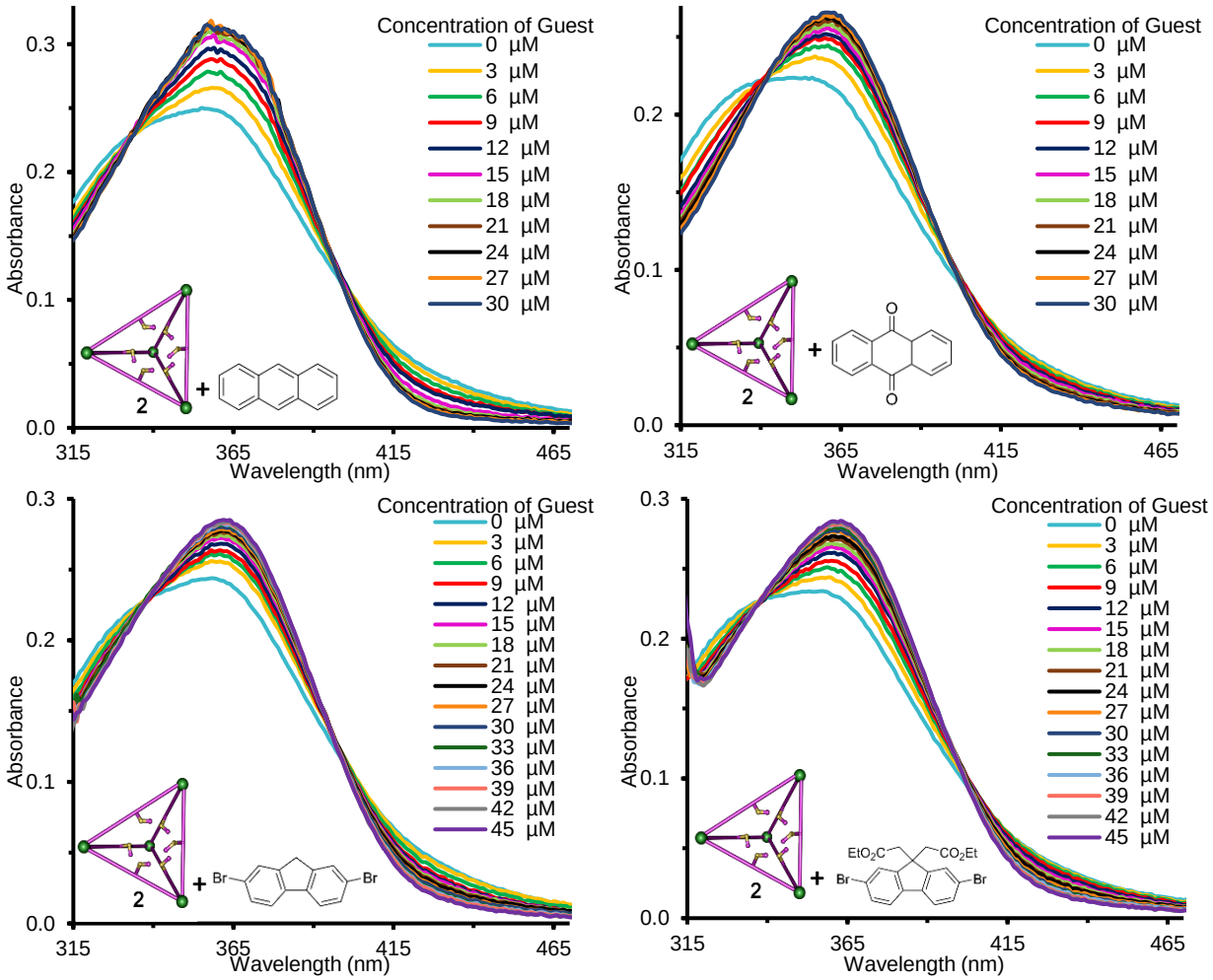

Figure *S-55.* UV-Vis absorption spectra of the titrations of guests **6–9** into 1 µM solutions of cage **2** in CH_3CN. Guests were added in 1 µL aliquots from a 9 mM stock solution in CH_3CN.

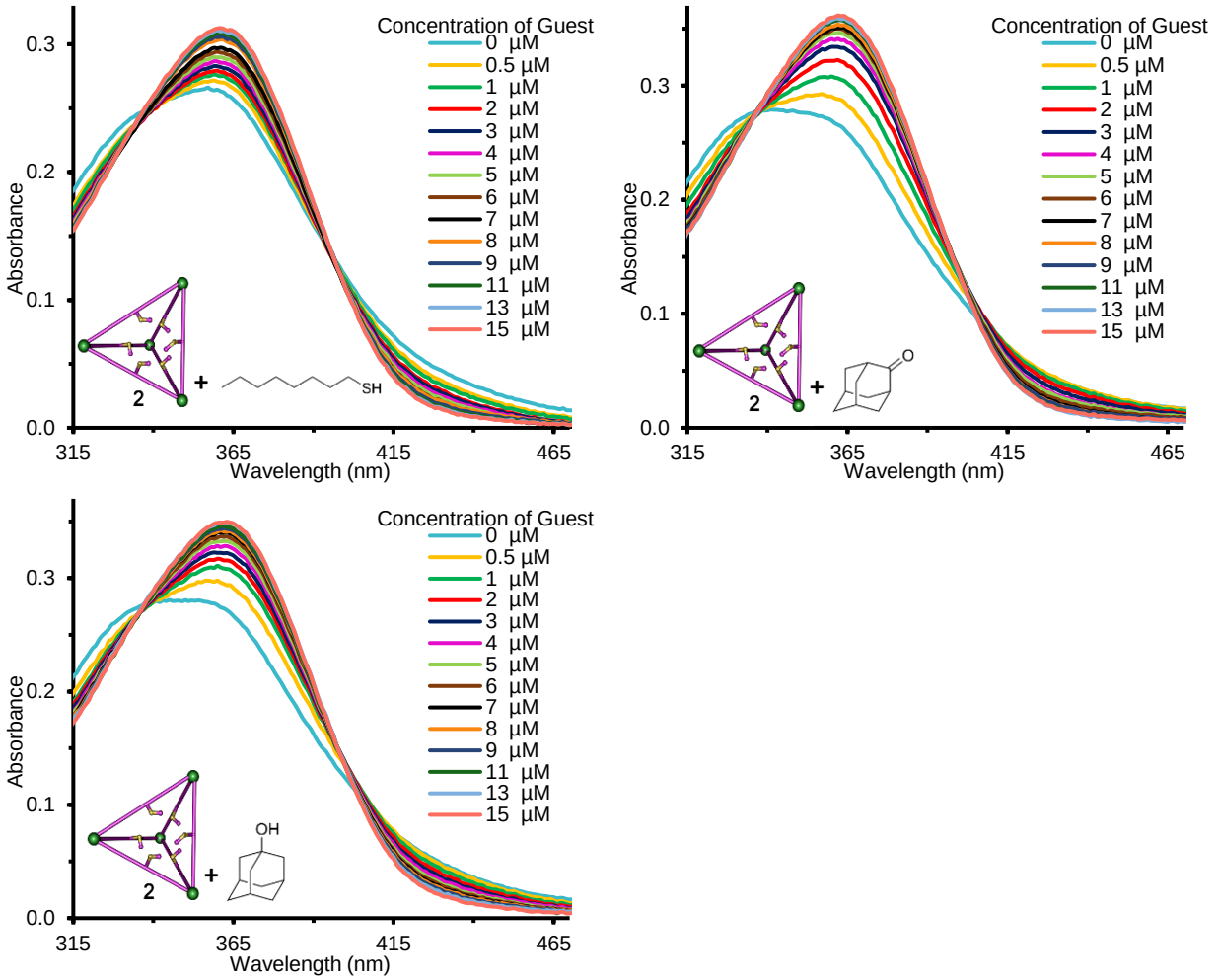

Figure *S-56.* UV-Vis absorption spectra of the titrations **10–12** into 1 µM solutions of cage **2** in CH_3CN. Guests were added in 0.5 and 1 µL aliquots from a 3 mM stock solution in CH_3CN.

UV/Vis Titrations of Guests into cage 3:

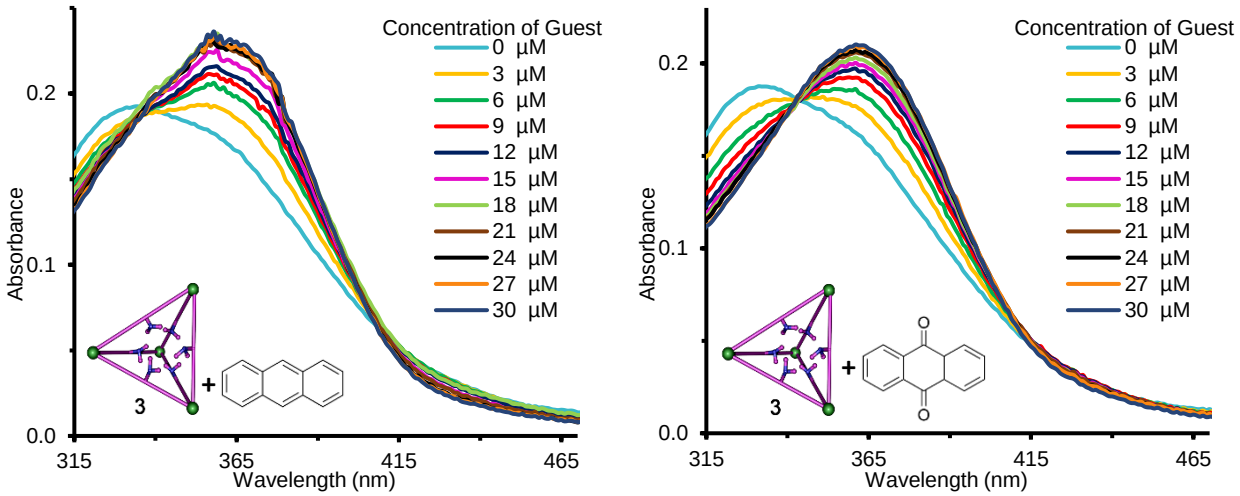

Figure *S-57.* UV-Vis absorption spectra of the titrations of **6** and **7** into 1 µM solutions of cage **3** in CH_3CN. Guests were added in 1 µL aliquots from a 9 mM stock solution in CH_3CN.

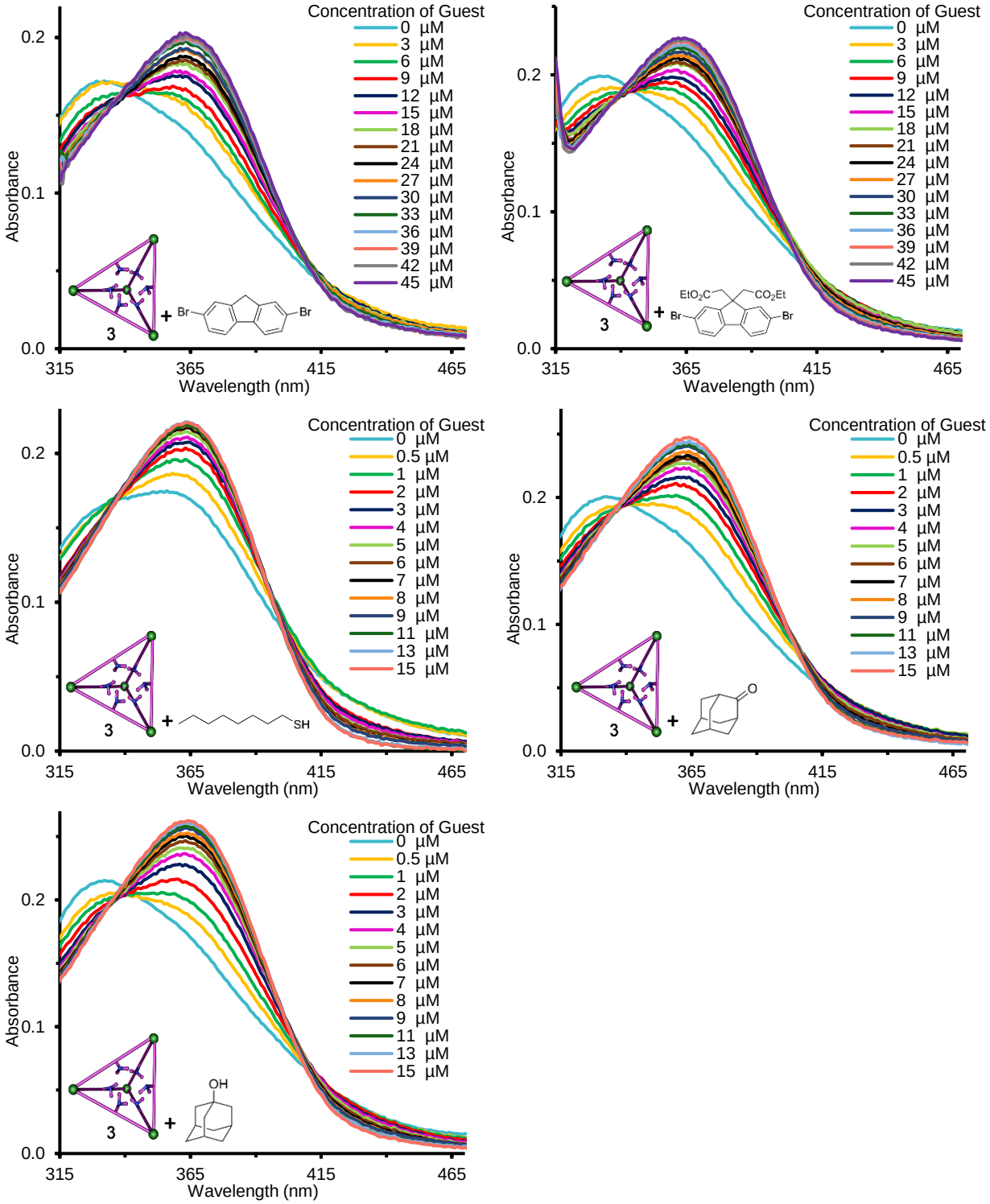

Figure *S-58.* UV-Vis absorption spectra of the titrations of **8–12** into 1 µM solutions of cage **3** in CH_3CN. Guests were added in 0.5 and 1 µL aliquots from a 3 and 9 mM stock solutions in CH_3CN.

UV/Vis Titrations of Guests into cages 4 and 5:

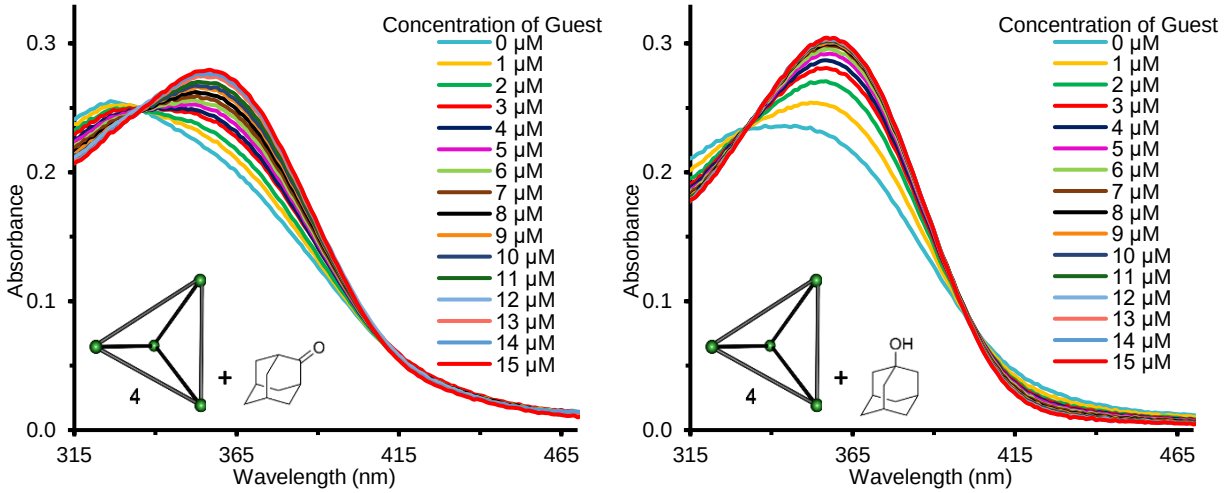

Figure *S-59.* UV-Vis absorption spectra of the titrations of **11** and **12** into 1 µM solutions of cage **4** in CH_3CN. Guests were added in 1 µL aliquots from a 3 mM stock solution in CH_3CN.

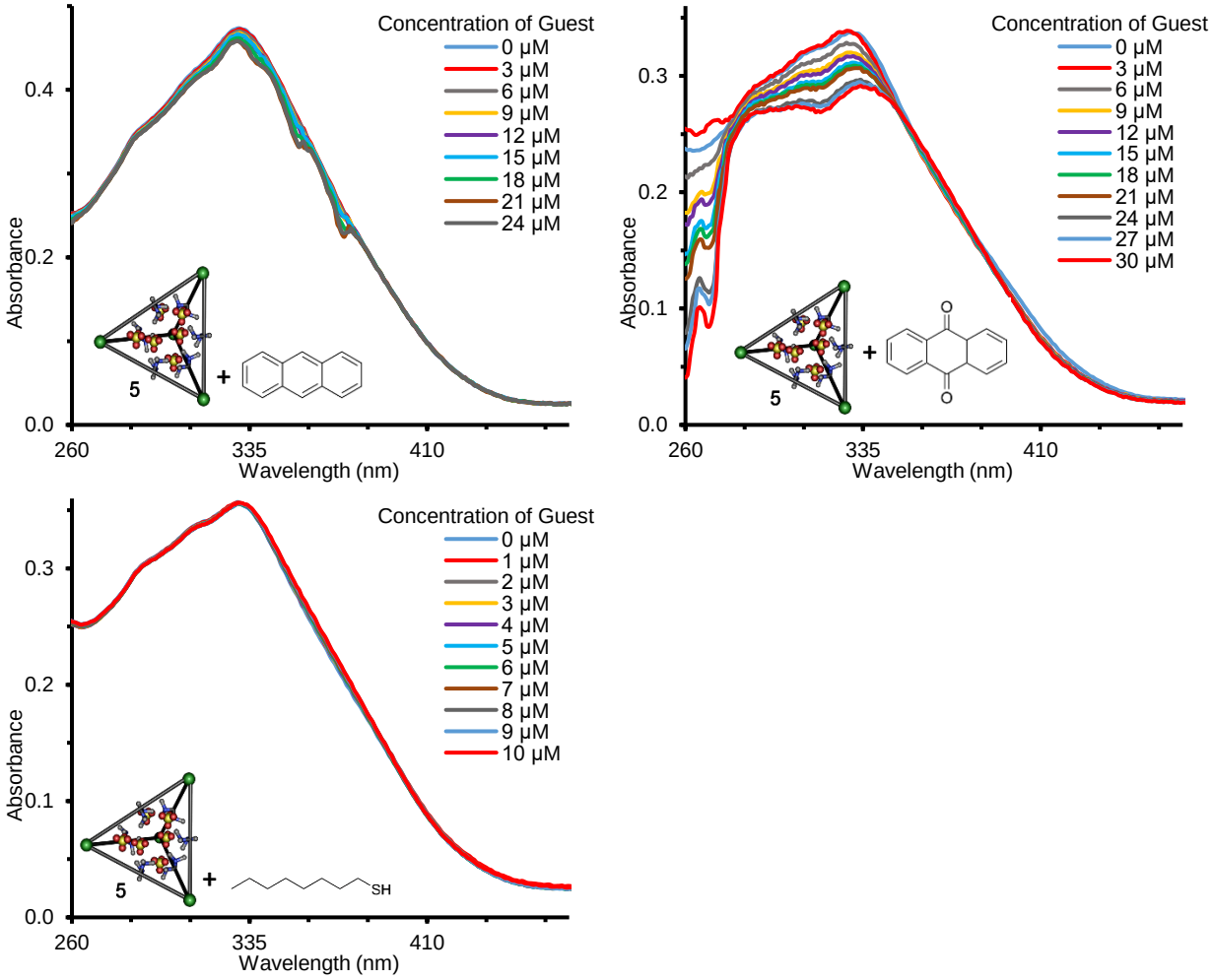

Figure *S-60.* UV-Vis absorption spectra of the titrations of **6**, **7**, and **10** into 1 µM solutions of cage **5** in CH_3CN. Guests were added in 1 µL aliquots from 3 and 9 mM stock solutions in CH_3CN.

IV. Acid and Base Binding

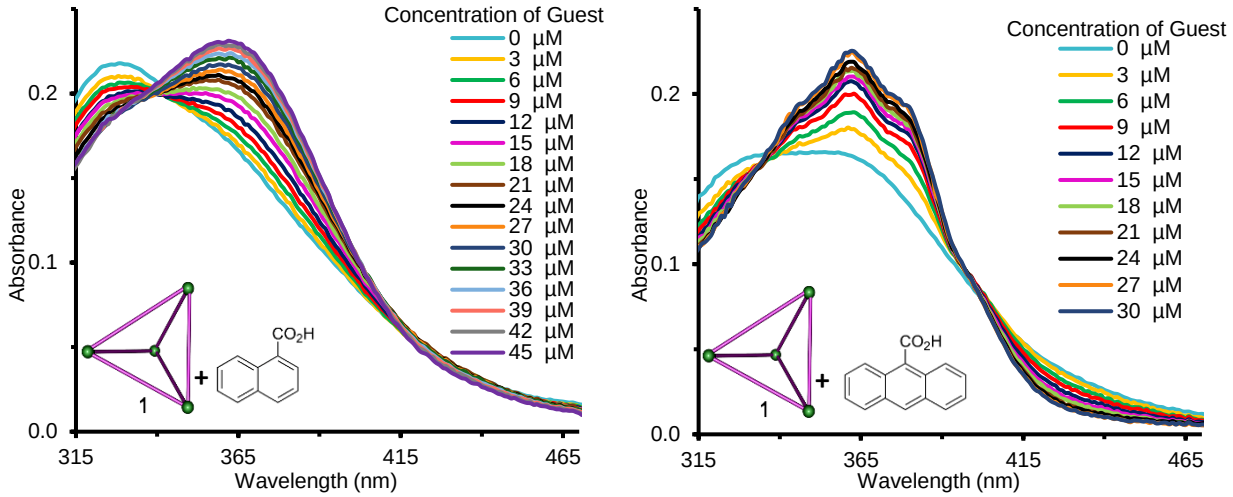

Figure *S-61.* UV-Vis absorption spectra of the titration of **13** and **14** into 1 µM solutions of cage **1** in CH_3CN. Guests were added in 1 µL aliquots from a 9 mM stock solution in CH_3CN.

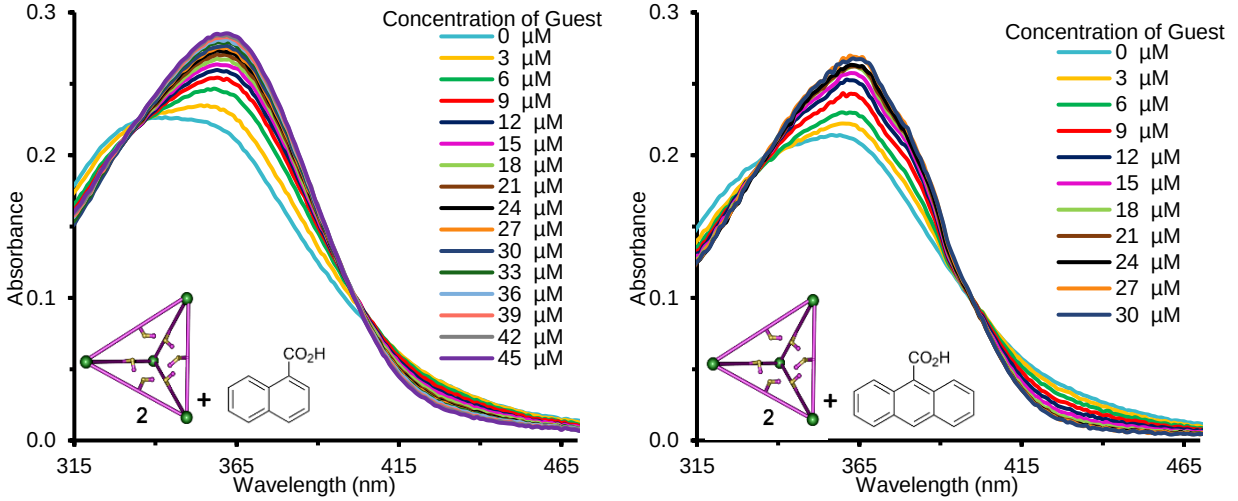

Figure *S-62.* UV-Vis absorption spectra of the titration of **13** and **14** into 1 µM solutions of cage **2** in CH_3CN. Guests were added in 1 µL aliquots from a 9 mM stock solution in CH_3CN.

3

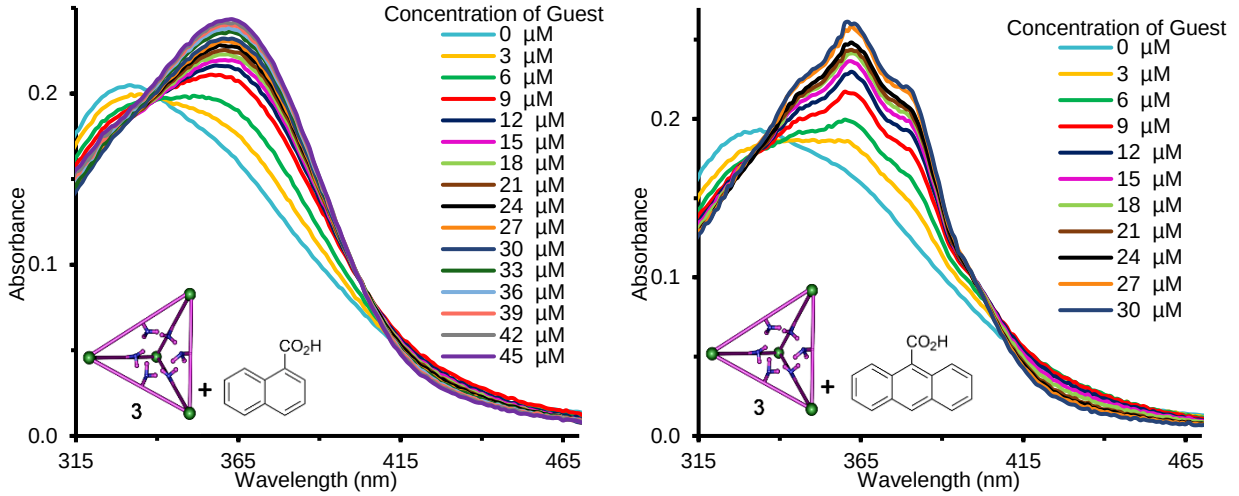

Figure *S-63.* UV-Vis absorption spectra of the titration of **13** and **14** into 1 µM solutions of cage **3** in CH_3CN. Guests were added in 1 µL aliquots from a 9 mM stock solution in CH_3CN.

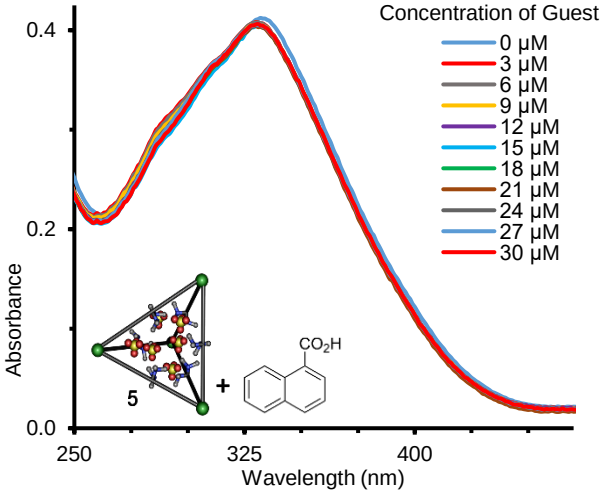

Figure *S-64.* UV-Vis absorption spectrum of the titration of **13** into 1 µM solutions of cage **5** in CH_3CN. Guest was added in 1 µL aliquots from a 9 mM stock solution in CH_3CN.

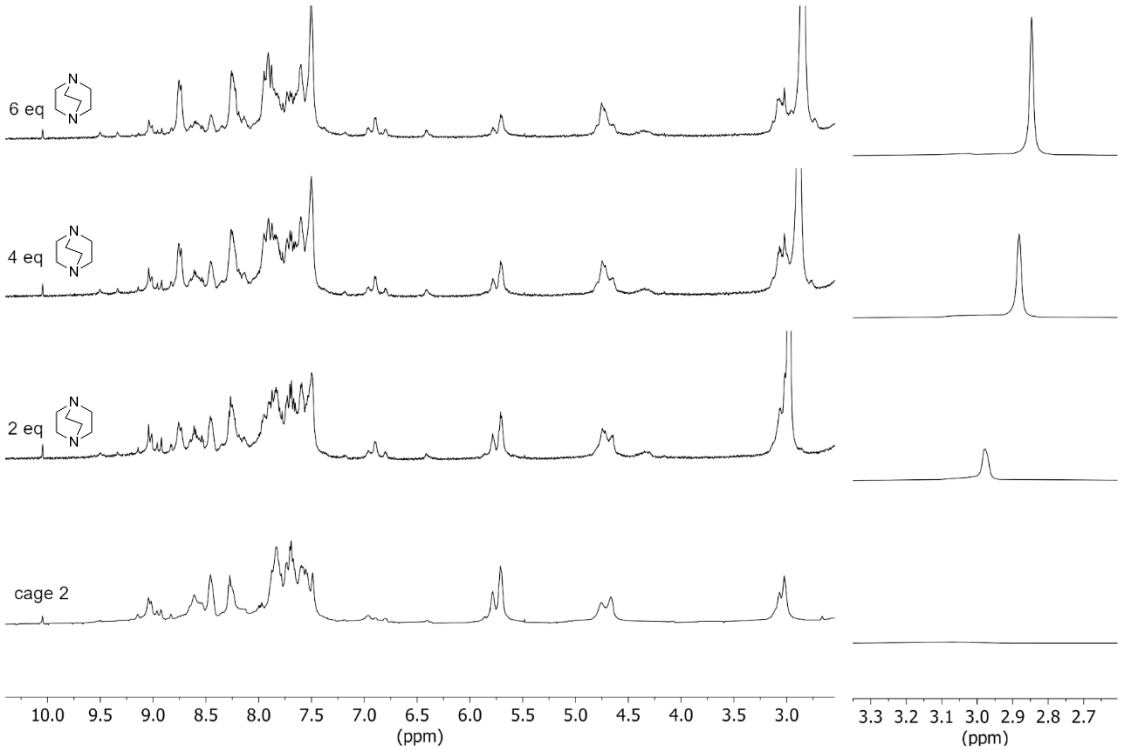

Figure *S-65.* ^{1}H NMR of the titration of DABCO into a 0.9 M solution of cage **2** in CD_3CN. DABCO was added in 1 µL aliquots from a 9 mM stock solution in CD_3CN.

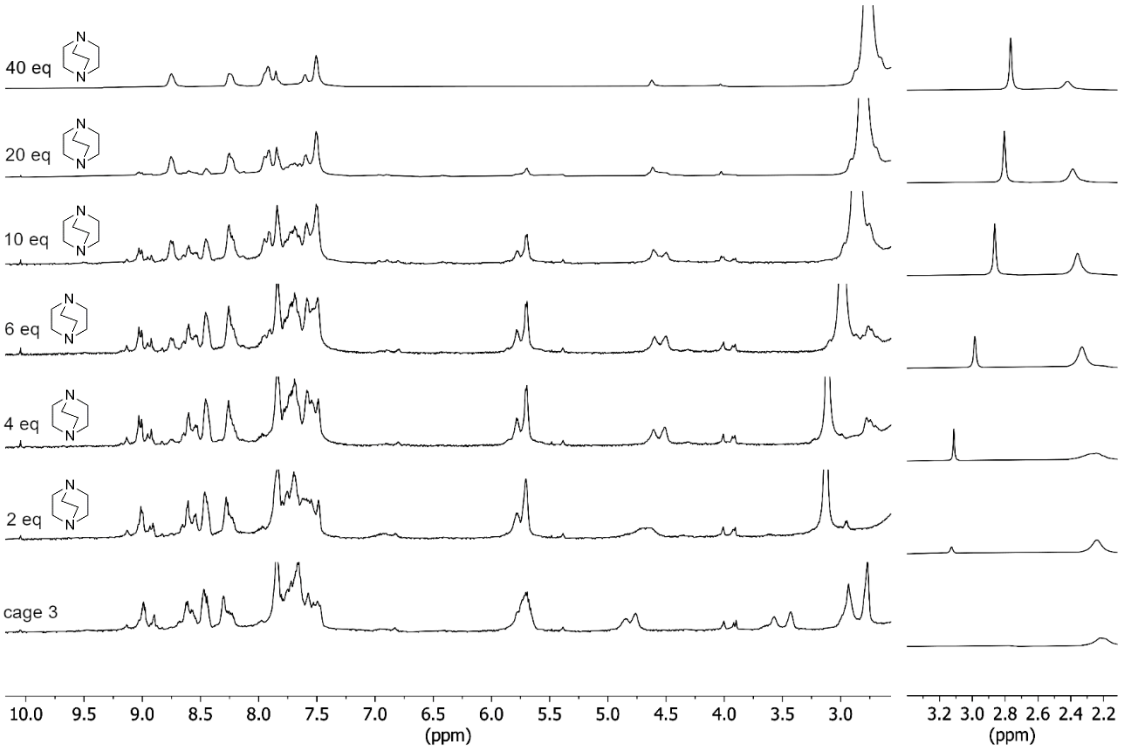

Figure *S-66.* ^{1}H NMR of the titration of DABCO into a 0.9 M solution of cage **3** in CD_3CN. DABCO was added in 1 µL aliquots from a 9 mM stock solution in CD_3CN.

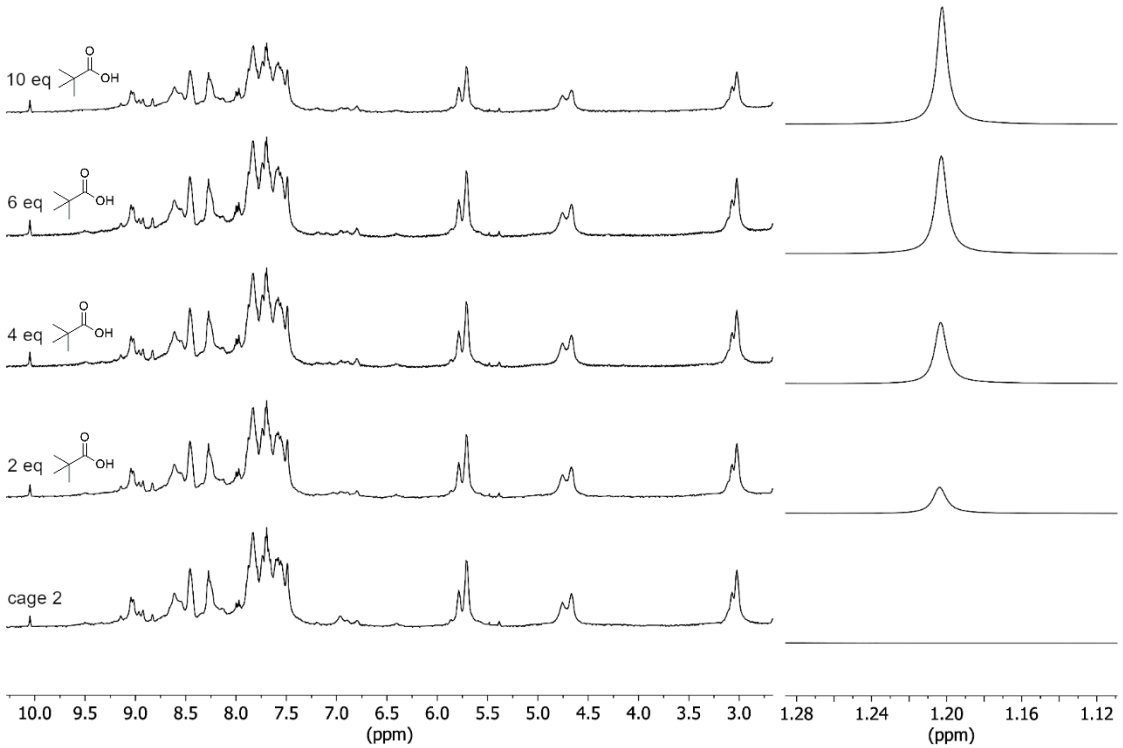

Figure *S*-*67*. ^{1}H NMR of the titration of pivalic acid into a 0.9 M solution of cage **2** in CD_3CN. Pivalic acid was added in 1 µL aliquots from a 9 mM stock solution in CD_3CN.

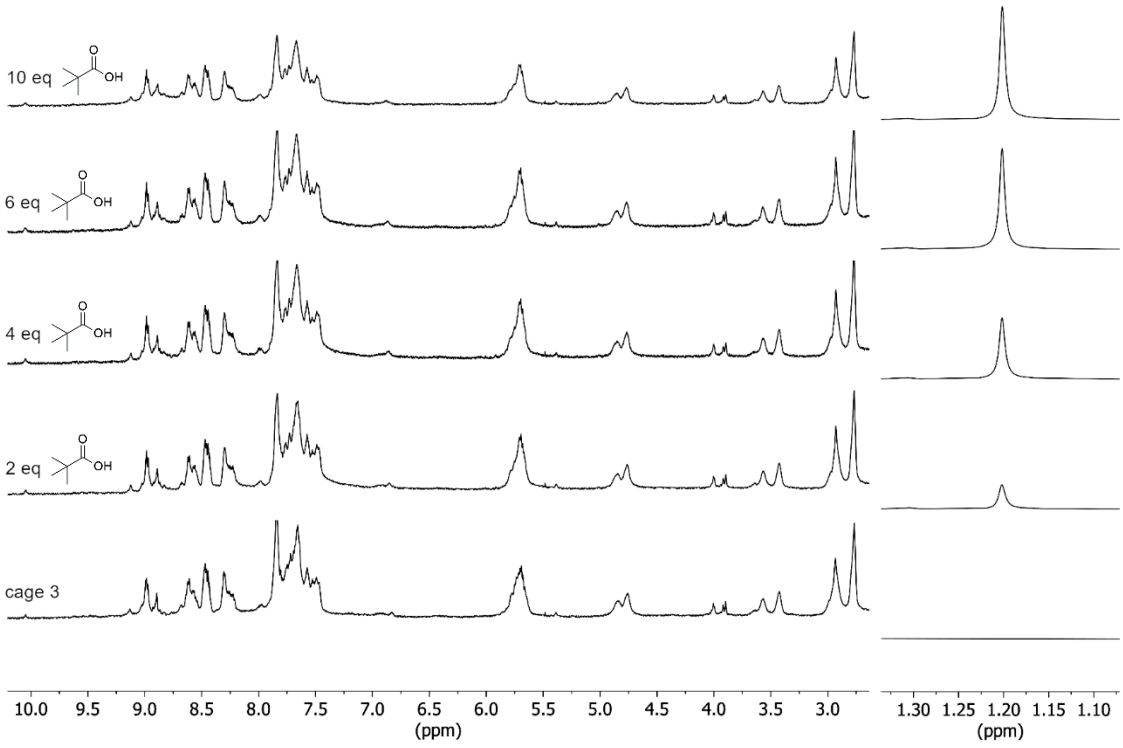

Figure *S*-*68*. ^{1}H NMR of the titration of pivalic acid into a 0.9 M solution of cage **3** in CD_3CN. Pivalic acid was added in 1 µL aliquots from a 9 mM stock solution in CD_3CN.

V. References

1. Association constants calculated using BindFit software found at http://supramolecular.org.
2. P. Thordarson, *Chem. Soc. Rev.* 2011, **40**, 1305−1323.
3. D. B. Hibbert, P. Thordarson, *Chem. Commun.* 2016, **52**, 12792−12805.